Ain Shams Engineering Journal 16 (2025) 103680

Contents lists available at ScienceDirect

Ain Shams Engineering Journal

journal homepage: www.sciencedirect.com

Full Length Article

Effect of steel and polypropylene fiber reinforcement on mitigating conversion effects in calcium aluminate cement at varying curing temperatures

Thwe Thwe Win [a], Yiwei Weng [b], Lapyote Prasittisopin [a,c,*]

[a] Centre of Excellence on Green Tech in Architecture, Department of Architecture, Faculty of Architecture, Chulalongkorn University, Bangkok, Thailand
[b] Department of Building and Real Estate, Faculty of Construction and Environment, The Hong Kong Polytechnic University, Hong Kong
[c] Department of Materials Science, Faculty of Science, Chulalongkorn University, Bangkok, Thailand

ARTICLE INFO

Keywords:
Polypropylene fiber
Steel fiber
Calcium aluminate cement
Fiber-reinforced composites
Curing temperature
Mechanical properties
Microstructural characteristics

ABSTRACT

Calcium aluminate cement (CAC) is widely used in high-performance applications due to its rapid setting and resistance to aggressive environments. However, its long-term durability is often compromised by hydration phase conversion, particularly under varying temperature conditions. At elevated curing temperatures, the conversion from metastable CAH_{10} and C_2AH_8 phases to the more stable, but porous, C_3AH_6 phase can lead to strength reduction. This study investigates how fiber reinforcement, specifically steel fibers (SF) and polypropylene fibers (PF), can mitigate these adverse effects in CAC composites cured at high temperatures (40 °C and 60 °C). A comprehensive evaluation of fiber-reinforced CAC composites was conducted, focusing on fresh and mechanical properties, chemical composition, and microstructural evolution. Experimental techniques included flowability, bulk density, void vol5me, water absorption, compressive strength, direct tensile strength, and flexural strength tests, complemented by X-ray diffraction (XRD), thermogravimetric analysis (TGA), and field emission scanning electron microscopy (FESEM) to assess phase composition and pore structure. The incorporation of fibers significantly enhanced the mechanical properties of CAC composites, with 1 % fiber addition improving compressive, direct tensile, and flexural strengths. At 40 °C, SF improved these strengths by approximately 26.5 %, 67 %, and 27.6 %, respectively, while PF enhanced them by 4.4 %, 24 %, and 16 %. However, at 60 °C, strength gains were less pronounced due to accelerated phase conversion and changes in porosity. Microstructural analysis reveals both SF and PF yield to reduced pore size, enhancing the strength and durability of the composites, attributed from the stable C3AH6 phase transition in CAC at higher curing temperatures up to 60 °C. This study provides new insights into the potential of fiber reinforcement in mitigating conversion-related strength loss in CAC at elevated temperatures. By enhancing mechanical performance and durability, SF and PF offer a sustainable approach to optimizing CAC composites for high-temperature applications, contributing to the development of eco-friendly, rapid-setting, and high-performance construction materials.

1. Introduction

A current challenge in cement and concrete production is to lower CO_2 emissions related to concrete manufacture. CAC has unique characteristics that make it highly desirable for use in high-temperature applications, leading to considerable interest in its qualities. Refractory materials and construction components exposed to high temperatures widely use it. CAC, due to its thermal stability, quick setting, and high strength, is an excellent option for environments that demand long-lasting and heat-resistant materials [1]. CAC possesses an exceptional capacity to quickly solidify and exhibit exceptional durability against chemical deterioration [2]. CAC is utilized in a wide range of particular applications that need remarkable resistance to high temperatures, superior strength at an early stage, and strong durability. Unlike regular Portland cement (OPC), which mainly uses the reactivity of calcium silicates, particularly tricalcium silicate (C_3S) and dicalcium silicate (C_2S), CAC has a very different hydration mechanism. CAC's main reactive phase, monocalcium aluminate (CA), plays a crucial role

* Corresponding author.
E-mail address: lapyote.p@chula.ac.th (L. Prasittisopin).

https://doi.org/10.1016/j.asej.2025.103680
Received 17 December 2024; Received in revised form 9 March 2025; Accepted 31 July 2025
Available online 25 August 2025

in its hydration, contributing significantly to early strength development. Notably, CA production results in only 48 % of the CO_2 emissions compared to C_3S [3], positioning CAC as an "eco-cement" and attracting considerable interest from both scientific and industrial researchers.

However, as hydration time continues, the strength of CAC gradually decreases due to a process called "conversion," as the microstructural porosity increases. How quickly metastable hydrates transform into more stable forms and what phases are formed are both heavily influenced by the temperature during hydration, accordingly to thermodynamically kinetics [4]. Upon hydration, CAC forms hexagonal phases like CAH_{10} and C_2AH_8 at room temperature (15–25 °C) [5], with C_2AH_8 gradually taking over as the temperature increases. When cured at 25–40 °C [6], C_2AH_8 becomes the primary hydration product, accompanied by alumina gel that eventually crystallizes into gibbsite (AH_3). The stable cubic phase C_3AH_6 and AH_3, which subsequently transforms into gibbsite, are formed at temperatures higher than 40 °C, and especially as the elevated temperature approaches 60 °C [7].

Thermodynamic **Eqs. (1) and (2)** [8] illustrate the inevitable transformation of metastable hydrates (CAH_{10} and C_2AH_8) into stable phases C_3AH_6 and AH_3. Conditions including time, heat, humidity, and pH play a role in this procedure. The conversion increases the paste's porosity and reduces its strength [5], posing significant challenges for the structural applications of CAC. Understanding and mitigating this conversion process are critical for the development of durable CAC-based materials [9,10]. The previous studies [5,6] showed that the incorporation of graphene nanoplatelets and fly ash into CAC composites greatly enhances their mechanical properties. The creation of silica tetrahedra in the CASH gel and the enhanced pore structure are responsible for the improvement. The results indicate a viable method for developing efficient and fast-setting concrete systems that are environmentally friendly.

$$3CAH_{10} \rightarrow C_3AH_6 + 2AH_3 + 18H \quad (1)$$

$$3C_2AH_8 \rightarrow 2C_3AH_6 + AH_3 + 9H \quad (2)$$

Micro-fibers have been widely utilized in concrete for improving their tensile strengths and durability. Traditional concrete, which has average strength, often has low resistance to tension and lacks flexibility. The use of fibers in concrete mixes can greatly enhance their mechanical characteristics, particularly their tensile strength [11–13]. The study conducted by Afroughsabet and Ozbakkaloglu [2] has demonstrated that the use of steel fiber (SF) and polypropylene fiber (PF), in conjunction with silica fume, can enhance the mechanical characteristics of high-strength concrete. In addition, the use of fibers in concrete decreases its water absorption and, depending on the type of fiber used, might modify its electrical resistance, enhancing the overall longevity of the concrete. In addition, a study conducted by Hussain et al. [14] showed that increasing the amount of SF in concrete decreases its water permeability, which is important for improving its durability.

The specially made setup accurately measures the water permeability when the material is directly pulled apart, showing that as the fiber dosages rise, the surface becomes rougher and the tortuosity decreases. In addition, PF have been employed with the aim of enhancing the fire resistance of concrete when subjected to high temperatures [15–17]. According to the recommendations of Pachideh et al. [15–17] and Gholhaki et al. [18] the main objective behind incorporating PF and SF into concrete is to mitigate the occurrence of extensive cracks under elevated temperature conditions. PF and SF serve as connectors between the cement paste and aggregates, strengthening the entire concrete structure and inhibiting the formation of wide cracks. Al-Sebai et al. [19] further developed constitutive models for macro synthetic fiber-reinforced concrete, enhancing the understanding of its mechanical behavior. Miftakhov et al. [20] advanced cloud-based research tools for polymer synthesis, offering valuable insights into fiber development. Furthermore, Nassif et al. [21] explored the durability of fiber-reinforced polymers, highlighting key challenges and innovations that are applicable to concrete fiber reinforcement. In this study, CAC's high-temperature resistance and rapid hardening are leveraged to improve the performance of fiber-reinforced composites. Fiber reinforcement, particularly with materials such as SF and PF, provides additional tensile strength and crack-bridging capabilities [7], which are crucial for enhancing the mechanical performance and durability of CAC composites. The combination of CAC's thermal stability and the reinforcing effects of fibers creates a composite material that maintains structural integrity and mechanical strength even under high-temperature curing conditions. Furthermore, high-temperature curing can accelerate the hydration process of CAC, leading to faster setting times and early strength gain, which are advantageous in construction scenarios where rapid turn-around is needed. However, the high curing temperature also poses challenges in terms of potential microstructural changes in the fiber-reinforced interface (ITZ) and the distribution of fibers within the matrix. This study investigates the interaction between CAC and fibers at elevated temperatures, with a particular focus on the resulting mechanical properties of the composite.

Without doubt, it is important to understand the conversion mechanisms of CAC with different fibers at higher curing temperatures where C_3AH_6 can thermodynamically form. The use of fiber reinforcement in CAC composites assume to be a promising in enhancing mechanical properties, yet its role under elevated curing temperatures remains underexplored, where the adverse conversion effects are more intensified. Based on the unexplored investigated stated above, the novelty of this study is to examine the SF and PF that were added to CAC matrices that were cured at elevated temperatures of 40 °C and 60 °C. The results provided useful information for scientists, engineers, and business owners who are working to improve the performance and longevity of CAC-based materials in extreme heat. Since there is a research gap on the impact of fibers on the mechanical characteristics of calcium aluminate cement at elevated curing temperatures, this study aims to find the rationales behind it. Consequently, a thorough evaluation was carried out to determine the impact of two different fibers, paying close attention to their mechanical qualities and microstructural features. Factors examined in this work entail water absorption, flowability, bulk density, volume of permeable voids (VPV), compressive strength, direct tensile strength, and flexural strength are considered. Further microstructural investigation into the CAC conversion process was carried out, entailing X-ray diffraction (XRD) and thermogravimetric analysis (TGA), and field emission scanning electron microscopy (FESEM). The findings point to the possibility of producing environmentally friendly, quick-setting, high-strength concrete systems through the development of CAC composites.

2. Materials and methods

2.1. Materials and mix proportions

2.1.1. CAC

The study employed Secar 71, a calcium aluminate cement manufactured by Kerneos. Its microstructural features were analyzed using scanning electron microscopy combined with energy-dispersive X-ray spectroscopy (SEM-EDS). This analysis indicated that the particles had different angular and asymmetrical forms, as seen in Fig. 1. Its chemical compositions, as displayed in Table 1, was determined by using X-ray fluorescence (XRF) (Bruker S8 Tiger).

2.1.2. Fibers

In this research, SF and PF were used to improve the strength of the CAC. The physical characteristics of these fibers, as outlined in their corresponding product data sheets, are provided in Table 2. Fig. 2 depicts the SF, which is straight and smooth and produced from wire that has been cold-drawn. SF has a 6 mm length, a 0.16 mm diameter, and a 37.5 aspect ratio, PF, on the other hand, has a length of 12 mm with its width ranging from 15–45 μm. Compared to PF, SF possesses higher

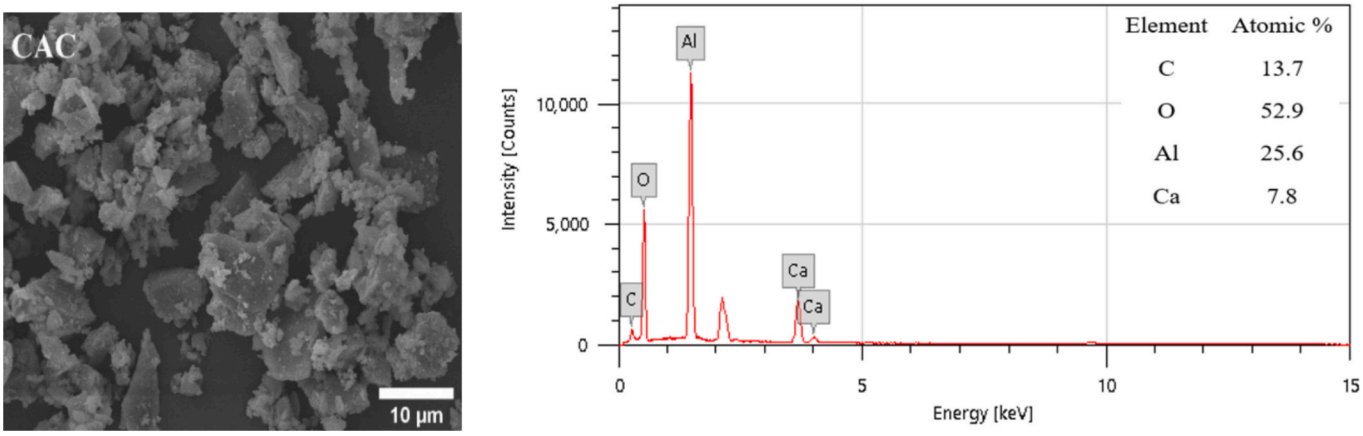

Fig. 1. SEM-EDS analysis of unhydrated CAC (SEM image captured at a magnification of 1000x with an accelerating voltage of 15 kV).

Table 1
Chemical and physical properties of CAC.

Chemical compositions (%)	CAC
SiO_2	0.25
Al_2O_3	66.01
Fe_2O_3	0.17
CaO	25.03
MgO	0.20
SO_3	8.10
Na2O	0.24
$SiO_2 + Al_2O_3 + Fe_2O_3$	66.43
LOI	0.62
Specific gravity (g/cm^3)	3.25
Blaine surface area (cm^2/g)	3919

Table 2
Properties of SF and PF.

Properties	SF	PF
Specific gravity	7.85	0.89–0.93
Fiber diameter (mm)	0.16	0.015–0.045
Fiber length (mm)	6	12
Modulus of Elasticity (GPa)	200	3.5
Tensile strength (MPa)	2750	340

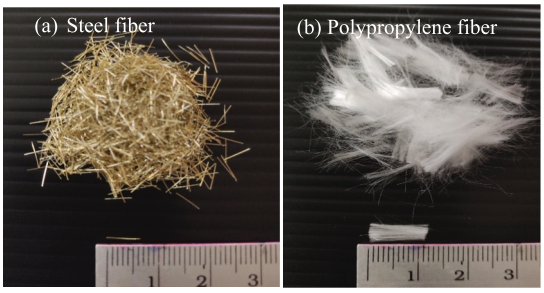

Fig. 2. Images of (a) SF and (b) PF.

density and tensile strength. These fibers are included in the composites in volume fractions of 1 % and 2 %. Preliminary testing was conducted with fiber contents of 1 %, 1.5 %, 2 %, and 2.5 %. The results indicated minimal differences in properties between 1 % and 1.5 %, while 1 % and 2 % fiber content demonstrated an optimal balance of properties in the mortar. As a result, 1 % and 2 % were chosen as the representative fiber contents for detailed investigation. In addition, the SF and PF mix ratios of 1 % and 2 % were chosen to balance workability and mechanical performance. Higher dosages can cause poor dispersion and agglomeration, affecting workability. Additionally, these ratios are widely used in similar studies for optimizing flexural strength and cost-effectiveness, ensuring consistency and comparability with existing research.

2.1.3. *Natural aggregate*

The fine aggregate utilized was natural river sand, purchased locally and carefully graded in accordance with the requirements set by ASTM C33 [22]. The sand possesses a specific gravity of 2.69 when it is saturated surface dry (SSD), an ability to absorb water of 0.71 %, and a fineness modulus of 2.79. Fig. 3 illustrates the distribution of particle sizes in the fine aggregate.

2.1.4. *Superplasticizer*

Superplasticizer is a substance that improves the fluidity and workability of concrete without sacrificing its strength. Sika® ViscoCrete®-2100, a construction chemical product from Sika, a company specializing in building chemicals, served as the superplasticizer in this study. This water-reducing additive, which utilizes polycarboxylate technology, enhances the workability of concrete mixtures, resulting in improved performance. The material exhibits a light brown color, is devoid of chloride, possesses a pH value of 4.96, and has a density of 1.061 g/cm^3. Uniformly spreading the fibers and minimizing clumping were essential for achieving this when combined with water. An amount of cement equal to 1 % of its weight was utilized to maximize the water-to-cement (w/c) ratio.

2.1.5. *Mixture proportions*

A control mortar mixture without fiber was prepared, following the guidelines of ASTM C109 [23]. Table 3 contains the specific ratios for five distinct mixtures, each containing varying amount of fiber (0 %, 1 %, and 2 %). Table 3 classifies the mixes based on their fiber compositions.

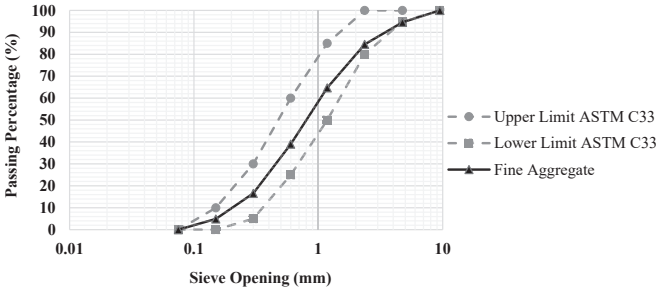

Fig. 3. Particle size investigation of fine aggregate.

Table 3
Mix proportions for fiber-reinforced CAC mortar.

Mixtures	CAC (g)	Sand (g)	Water (g)	Superplasticizer (%)	Fiber	
					Type	Volume content (%)
Control	100	275	55	1	–	0
SF1	100	275	55	1	SF	1
SF2	100	275	55	1	SF	2
PF1	100	275	55	1	PF	1
PF2	100	275	55	1	PF	2

2.2. Sample preparation assessment

Mixing procedure of CAC mortars in this work was outlined in ASTM C305 [27]. After meticulous measurement, the exact amounts of fibers, CAC, and fine aggregate were added in a mechanical mixer for up to a minute. Subsequently, water and a superplasticizer were introduced, and the wet-mixing was carried out for around 3 min to achieve a uniform mixture.

Special attention was given to ensuring an even dispersion of PF throughout the mixture. Precise management of the mixing procedure was necessary. A high-velocity mixer was performed to guarantee complete amalgamation of the fibers with the rest of the ingredients. The inclusion of the superplasticizer enhanced the mixture's workability, facilitating the more efficient dispersion of the fibers inside the composite. Systematic modifications were implemented to the mixing settings, including mixing duration and speed, in order to prevent the agglomeration of fiber [28]. This ensured a uniform distribution of fibers and consistent mechanical properties in all samples to achieved optimal strengths and durability.

After achieving uniform consistency, the fresh mortar mix was instantly assessed for its immediate characteristics. The workability of the fresh mortar was assessed by performing the flow table test, in accordance with the instructions outlined in ASTM C1437 [29]. After mixing the materials, the fresh mortar was poured into molds and maintained at a constant temperature of 23 ± 2°C, with a humidity level of above 95 %, for a period of 24 h. Following their removal from the molds, the specimens underwent curing at elevated temperatures of 40 °C and 60 °C [30] for mechanical performance tests, as shown in Fig. 4. The selection of 40 °C and 60 °C was based on the distinct hydration behavior of CAC at elevated temperatures, as explained in the Introduction section. Previous studies [7] have shown that at room temperature (15–25 °C), CAC hydration predominantly forms hexagonal phases like CAH_{10} and C_2AH_8. As temperatures increase to the range of 25–40 °C, C_2AH_8 becomes the dominant phase, accompanied by the formation of alumina gel, which eventually crystallizes into gibbsite (AH_3). When temperatures exceed 40 °C and approach 60 °C, stable cubic phases such as C_3AH_6 and AH_3 begin to form, signaling a shift in the hydration mechanism. This temperature-dependent phase transformation was the basis for choosing 40 °C and 60 °C, to specifically investigate how higher curing temperatures affect the hydration process, with a focus on phase stability and resulting strength characteristics.

2.3. Methods of characterization

This study was designed to evaluate the effects of fiber reinforcement on the mechanical and microstructural properties of CAC mortar cured at elevated temperatures (40 °C and 60 °C) for 7- and 28-day (in Table 4). Five distinct mortar compositions were prepared to systematically investigate the influence of steel fibers (SF) and polypropylene

Fig. 4. Flow chart of the mixing process and sample preparation.

Table 4
Detailed properties of hardened mortar under experimental conditions.

Properties	Reference	Dimension and shape	Water curing age (days)	Curing temperature (°C)
Bulk density	ASTM C642 [24]	50 mm-cube	28	40,60
VPV	ASTM C642 [24]	50 mm-cube	28	40,60
Water absorption	ASTM C642 [24]	50 mm-cube	28	40,60
Compressive strength	ASTM C109 [23]	50 mm-cube	7, 28	40,60
Direct tensile strength	Monaco et al. [25]	500 mm^2-briquette cross-sections	28	40,60
Flexural strength	ASTM C348 [26]	40 × 40 × 160 mm^3-beam	28	40,60

fibers (PF). The primary properties analyzed included bulk density, void percentage (VPV), water absorption, compressive strength, direct tensile strength, and flexural strength, as they are key indicators of the mechanical performance and durability of fiber-reinforced CAC composites, especially under elevated curing temperatures. These parameters directly influence the material's structural integrity, resistance to degradation, and overall longevity, which are crucial for high-temperature applications. Additionally, phase composition and microstructural characteristics were examined using XRD, TGA, and FESEM to assess how fiber incorporation affects mechanical performance and phase transformation under high-temperature curing conditions.

The experimental procedure involved preparing mortar mixtures following standardized mixing protocols to ensure consistency in material proportions, mixing time, and casting [31]. Specimens were molded into cubic samples (50 × 50 × 50 mm) for compressive strength testing, briquette specimens (minimum cross-section of 500 mm^2) for direct tensile strength testing, and beam specimens (40 × 40 × 160 mm^3) for flexural strength testing. For each mix ratio and curing temperature, three samples were prepared and tested to obtain an average value, ensuring accuracy and consistency in the experimental results. Mechanical strength tests were conducted following standardized methods, with compressive strength evaluated according to ASTM C109/C109M [23], tensile strength measured based on Monaco et al. studied [25], and flexural strength determined using ASTM C348 [26].

For phase and microstructural analysis, XRD, TGA, and FESEM techniques were employed. XRD analysis was conducted using a BRUKER D8 DISCOVER instrument set at 40 kV and 30 mA, utilizing Cu Kα radiation with a wavelength of 0.154 nm. Data were collected over a 2θ range of 5–80°, with a step size of 0.02° and a duration of 0.5 s per step. The crystalline phases were identified through qualitative analysis. Qualitative analysis was performed by comparing the diffraction patterns with reference data obtained from established literature and the International Centre for Diffraction Data (ICDD) database, ensuring accurate phase identification. Additionally, XRD analysis was conducted on samples cured at different temperatures to investigate the transformation of metastable hydrates into stable phases, offering insights into the effects of curing conditions on phase development. TGA analysis was carried out using a Perkin Elmer Pyris 1 instrument, where samples were heated from 25 °C to 1000 °C at a controlled rate of 10 °C per minute in a nitrogen atmosphere at a flow rate of 70 ml per minute. This method provided insights into phase transformations and hydration conversion in CAC. Additionally, microstructural characterization was performed using a Quanta 250 FEG FESEM to observe fiber dispersion, matrix bonding, and pore structure. Specimens were collected from 7- and 28-day cured samples, dried, cleaned, coated with gold, and mounted on copper studs using carbon tape for imaging.

Data analysis was conducted systematically to ensure accuracy and reliability. Mechanical properties were averaged from three independent measurements per test condition. XRD results were interpreted qualitatively by identifying diffraction peaks and comparing them with reference patterns. TGA mass loss trends were examined to determine hydration phase transitions and thermal stability, while FESEM images provided microstructural insights into the effects of fiber incorporation on pore structure and matrix bonding. Figs. 5 and 6 illustrate the experimental workflow.

3. Results and discussion

3.1. Workability of fresh mortar

The ability to place and manipulate mortar easily is an essential attribute. The findings of the flow table test, which assesses the workability of different mortar mixes, are shown in Table 5. The control mortar (100 % cement) had the highest degree of workability, as evidenced by a flow value of 139 %. Nevertheless, the incorporation of fibers led to a substantial decrease in workability. SF- and PF-CAC mortars have flow values ranging from 115–120 % and 41–65 %, respectively (see Fig. 7**a**). An observed association was found: the level of difficulty in dealing with the material decreased as the quantity of fiber increased. Specifically, the proportion of SF in the volume increased from 1 % to 2 %, resulting in a decrease in workability by 14 % and 17 %, respectively. Concerning PF, there was a significant decrease in workability, with a decline of 53 % at 1 % fiber content and 71 % at 2 %. The latter value, when compared to the control sample, shows the lowest workability among all the fiber-reinforced mortars. The interactions between the cement paste and fiber surfaces likely cause the decrease in workability associated with PF. These observations were consistent with the previous study [32]. Nevertheless, Nuaklong et al. [33] found that the workability of concretes remained unchanged regardless of the type or amount of fiber employed. They observed that the slump flows remained within a reasonably narrow range, suggesting no significant deviations. Despite variations in workability, the mortar mixtures consistently retained enough workability to effectively disperse particles. The fibers make the mixture less workable because they weave together with the cement grains and small aggregate particles to make a network that makes the mixture less likely to flow. Furthermore, the inclusion of fibers increases the interior surface area and interparticle friction, leading to a more pronounced reduction in workability.

3.2. Physical properties

3.2.1. Bulk density

This study evaluated the bulk density of fiber-reinforced CAC mortar after a 28-day curing period at two different temperatures, 40 °C and 60 °C. According to the data given in Fig. 7**(b)**, the inclusion of SF and PF in the mixture significantly increased its density compared to the control mixture, which did not contain any fibers. As a result, CAC undergoes hydration to become C_3AH_6 and AH_3, hence developing porosity [34]. Specifically, at 40 °C, the addition of 1 % SF resulted in a bulk density increase of 3.3 %, reaching 2221 kg/m3, while 2 % SF contributed to a 2.8 % increase, with a bulk density of 2210 kg/m3. The increase was attributed to the high specific gravity of SF and its ability to prevent crack formation, thereby reducing void content. In addition, at a lower fiber content of 1 %, the fibers distribute more effectively throughout the matrix, facilitating a more efficient packing of hydration products like calcium aluminate hydrates (CAH) and monosulfoaluminate (AFm) phases, leading to a higher bulk density of 3.3 %. At 2 % SF, on the other hand, the higher fiber content may make packing less effective because fibers may stick together or stop hydration products from forming around the fibers. This is why the density only went up by 2.8 %. Similarly, the inclusion of PF at 1 % and 2 % led to increases of 1.4 % and 0.5 %, respectively, highlighting the fibers' role in void reduction. At an elevated temperature of 60 °C, the trend persisted, with the 1 % SF and

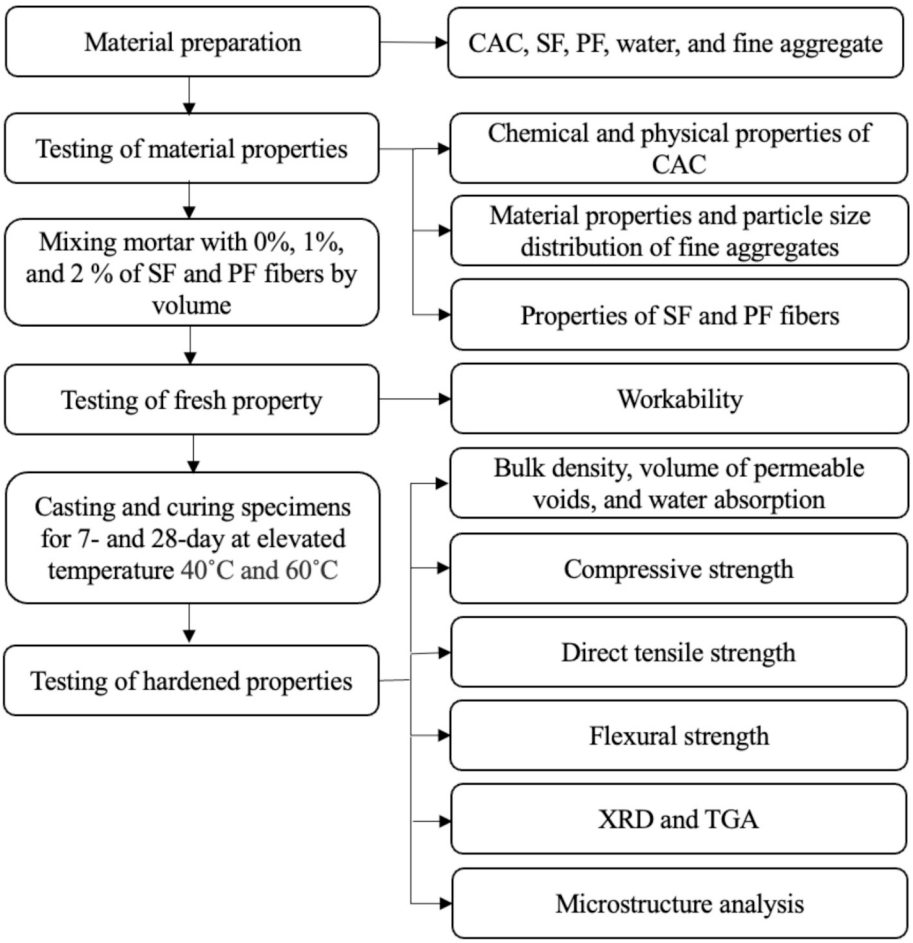

Fig. 5. Experimental design configuration.

2 % SF dosages resulting in bulk density increases of 3.5 % and 2.8 %, respectively. The PF-enhanced samples at 60 °C showed increases of 1.0 % and 0.5 % for 1 % and 2 % dosages, respectively. These results show that fiber reinforcement and curing temperature have an effect on how dense CAC mortar gets. This is in line with other research that showed that adding fibers increased density and decreased void content [35,36].

Moreover, our previous study [7] at ambient temperature showed a consistent trend, where the addition of SF and PF similarly resulted in increased bulk density. This suggests that the densification effect of fibers is robust across a range of curing temperatures. Interestingly, the bulk density of CAC mortar cured at 60 °C is generally less than that at 40℃ due to the conversion process, but it is still significantly higher than that of the control sample. The conversion process at 60 °C involves the transformation of metastable hexagonal hydrates into stable cubic phases, which typically results in a denser microstructure. However, the higher temperature also accelerates hydration, leading to a more complete reaction and overall densification. Therefore, the fiber-reinforced mortar that was cured at 60 °C is still denser than the control, even though it is less dense than the sample that was cured at 40 °C. This shows that fiber reinforcement can increase bulk density even at higher curing temperatures. The pattern in density formation that has been observed is in line with the mechanical properties of CAC composites, which include fibers.

3.2.2. *Volume of permeable voids*

With regard to the durability of material, Table 5 provides an illustration of how different fiber contents affect the VPV in mortar samples that were cured for 28 days at 40 °C and 60 °C. A negative correlation was shown between the amount of fiber and VPV, as VPV decreased when fiber content increased from 0– 2 %. At a temperature of 40 °C, the presence of SF caused a decrease in VPV of 21.8 % in the SF1 mixture and 16.5 % in the SF2 combination, compared to the control. This is consistent with research findings that indicate SF function as crack arresters, hence decreasing the permeability of concrete by impeding the spread of cracks in hardened concrete [37]. Similarly, the mixes reinforced with PF, known as PF1 and PF2, demonstrated decreases in VPV of 14.4 % and 12.67 % correspondingly. This indicates that PF is effective in lowering permeability.

As shown in Fig. 7**(c)**, at a higher temperature of 60 °C, the influence of SF on VPV remained substantial, but less noticeable compared to the impact at 40 °C. The SF1 and SF2 combinations exhibited decreases in VPV of 17.1 % and 8.9 %, respectively. The combinations of PF1 and PF2 also showed reductions in VPV, with drops of 7.3 % and 5.0 % respectively, compared to the control mixture. The results are confirmed by previous research [38] and are corroborated by the microstructural examinations reported in **Section 3.6**, which demonstrate enhancements in pore structure, decreased porosity, and improved densification. While the VPV values at 60 °C were greater than those at 40 °C, suggesting a less compact structure resulting from the conversion process of CAC, they nevertheless remained considerably lower than the control sample, emphasizing the advantageous impact of adding fiber. When compared to prior research [7] done at room temperature, the VPV values for SF1 and SF2 combinations reduced by 23.8 % and 6.8 % respectively. Similarly, the PF1 and PF2 mixtures had reductions of 5.9 % and 3.8 % respectively. The continuous decrease in VPV at various temperatures highlights the efficacy of fiber reinforcing.

By including SF and PF, the mechanical qualities of the mortar are improved, as explained in **Section 3.3**. Additionally, this also increases

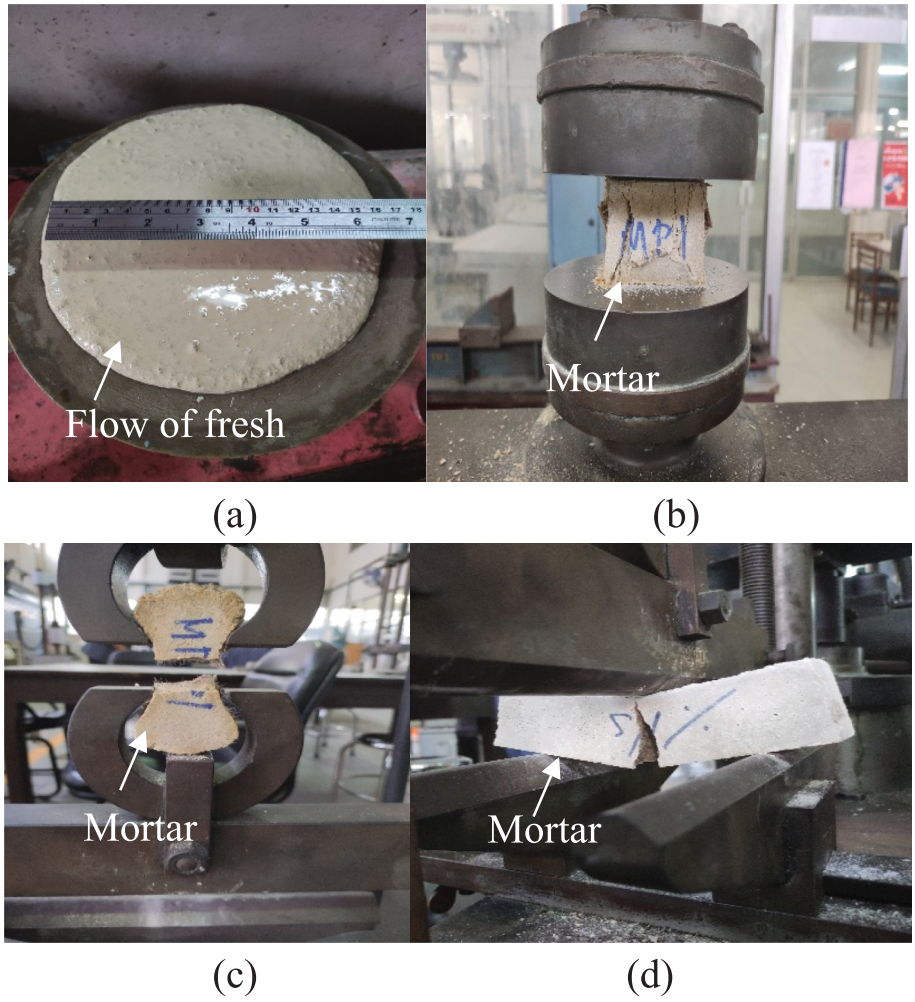

Fig. 6. Experimental protocol: (a) Flowability measurement, (b) Compressive strength test, (c) Direct tensile strength test, and (d) Flexural strength test.

Table 5
Physical properties data.

Mix	Physical characteristics (28-day)*						
	Flow (%)	Bulk density (kg/m^3)		VPV (%)		Water absorption (%)	
		40 °C	60 °C	40 °C	60 °C	40 °C	60 °C
Control	139 ± 1.15	2150 ± 0.007	2130 ± 0.006	9.86 ± 0.14	11.12 ± 0.12	5.10 ± 0.14	7.14 ± 0.10
SF1	120 ± 0.58	2221 ± 0.003	2205 ± 0.004	7.71 ± 0.17	9.22 ± 0.10	4.12 ± 0.08	5.21 ± 0.08
SF2	115 ± 0.58	2210 ± 0.008	2190 ± 0.008	8.23 ± 0.10	10.13 ± 0.13	4.42 ± 0.06	5.64 ± 0.07
PF1	65 ± 0.55	2180 ± 0.003	2150 ± 0.004	8.44 ± 0.09	10.31 ± 0.21	4.54 ± 0.13	6.10 ± 0.12
PF2	41 ± 1.11	2160 ± 0.005	2140 ± 0.002	8.61 ± 0.11	10.56 ± 0.14	4.73 ± 0.20	6.43 ± 0.06

*Data show mean value ± standard deviation.

the long-term endurance of the construction. The enhanced durability of the building provides environmental benefits by minimizing the requirement for frequent repairs or replacements. This, in turn, advocates conserving materials, reducing pollution, lowering energy consumption and lessening negative social impacts during the lifespan of the construction [13,39].

3.2.3. *Water absorption*

Fig. 7**(d)** exhibits the results of the water absorption test for CAC composites, which included fibers and underwent curing at 40 °C and 60 °C. The water absorption test quantifies the VPV attached to the surface of concrete. This parameter is important for assessing the durability of the concrete because it determines the extent to which dangerous chemicals can leak through the surface. After a 28-day curing period at both temperatures, the incorporation of SF and PF into the mortar notably reduced water absorption, suggesting improved durability due to decreased porosity.

Particularly, the experimental data suggested that the addition of SF significantly reduced water absorption. At 40 °C, the water absorption values for the SF1 and SF2 mixtures were 4.12 % and 4.42 %, respectively, representing reductions of 19.2 % and 13.3 % compared to the control mixture. This decrease in water absorption is in line with prior research on conventional concrete [38], which found that SF can limit crack propagation, leading to a denser microstructure. The reduced water absorption in SF-containing mixes compared to those without SF indicates enhanced performance, particularly in terms of resistance to the ingress of potentially harmful substances [37]. Incorporating PF also reduced the mixtures' water absorption capacity. The water absorption values of the PF1 and PF2 mixtures were 11.0 % and 7.25 % lower, respectively, compared to the mixes without PF, which had values of 4.54 % and 4.73 %.

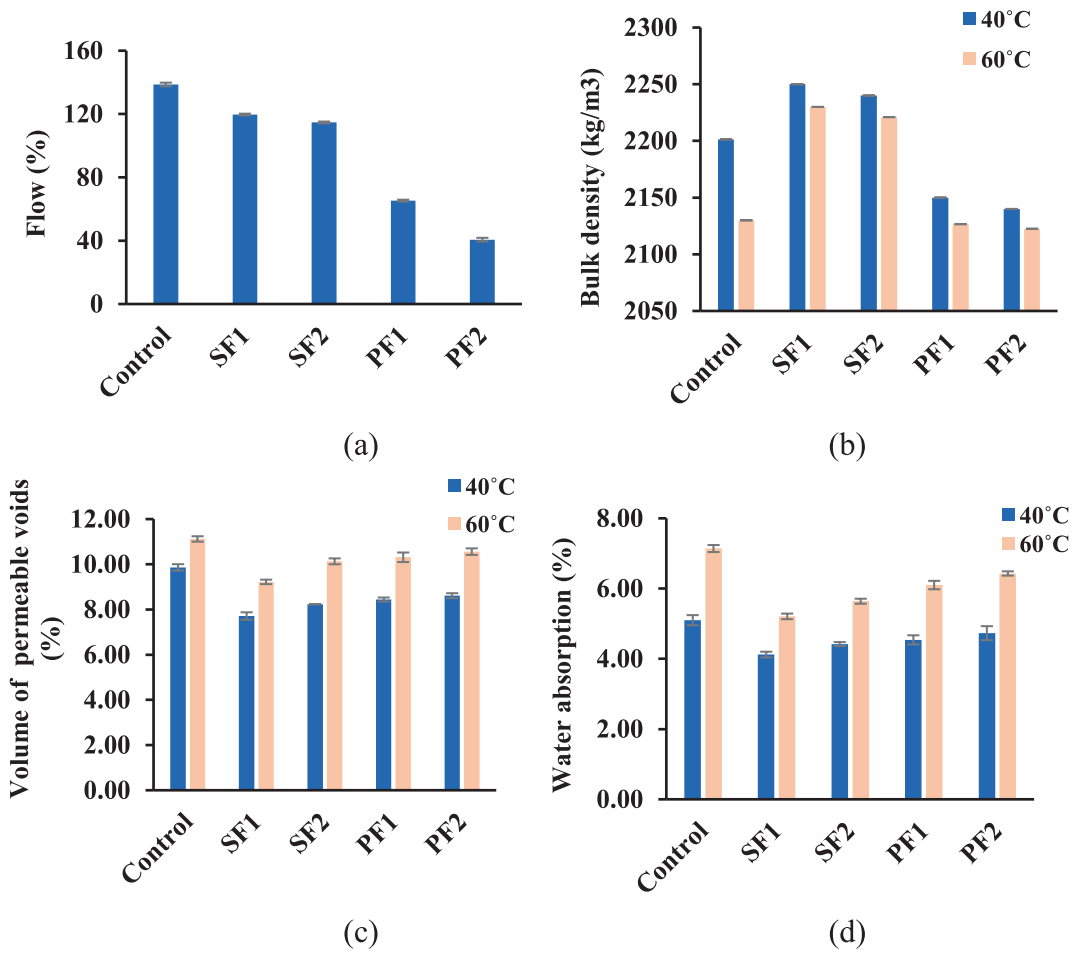

Fig. 7. Physical characteristics of CAC mortar including SF and PF: (a) flow; (b) density; (c) VPV; and (d) water absorption.

At a higher temperature of 60 °C, the SF1 and SF2 mixes showed much greater decreases in water absorption. The water absorption values for SF1 and SF2 were 27 % and 21 % lower, respectively, compared to the control combination. This resulted in water absorption values of 5.21 % and 5.64 % for SF1 and SF2, respectively. The PF1 and PF2 blends exhibited decreases of around 14.6 % and 10.0 %, respectively. While the water absorption values at 60 °C were generally higher than those at 40 °C, suggesting a less compact structure resulting from the conversion process of CAC, they were still much lower than the control sample. These findings indicate that when the conversion process occurs at a temperature of 60 °C, where metastable hexagonal hydrates are transformed into stable cubic phases, it generally leads to a more compact microstructure, even though there is greater water absorption.

Before doing this experiment, we discovered that at normal room temperature, the SF1 and SF2 mixtures had a lower water absorption rate in comparison to the control combination, with reductions of 14.7 % and 11.1 %, respectively. Both the PF1 and PF2 mixtures decreased their water absorption efficiency by 8.6 % and 5.9 %, correspondingly [7]. Upon comparing these data to the present investigation, it is clear that the decrease in water absorption at 40 °C is more noticeable than at room temperature, suggesting that the fibers are more effective in lowering porosity at higher temperatures. At a temperature of 60 °C, the reduction percentages are even more elevated for SF mixes, although slightly lower for PF mixes in comparison to 40 °C. Still, they significantly outperform the control.

Fig. 8 illustrates a direct correlation between water absorption and VPV, indicating that when VPV values increase, water absorption also increases. The high correlation obtained, as evidenced by a R^2 value of 0.92, highlights the dependency between these two metrics. Therefore, the addition of fibers leads to reduced water absorption, which is consistent with the VPV data. Including SF and PF in CAC mortar makes it stronger and last longer by making it less porous and able to absorb water. This enhances the longevity of structures and improves their environmental impact by minimizing the necessity for regular repairs or replacements. These findings emphasize the significance of using fiber reinforcement to enhance the performance of CAC composites across different curing conditions. Furthermore, when compared to prior studies conducted at normal room temperature, it is evident that higher curing temperatures, especially around 40 °C, amplify the positive

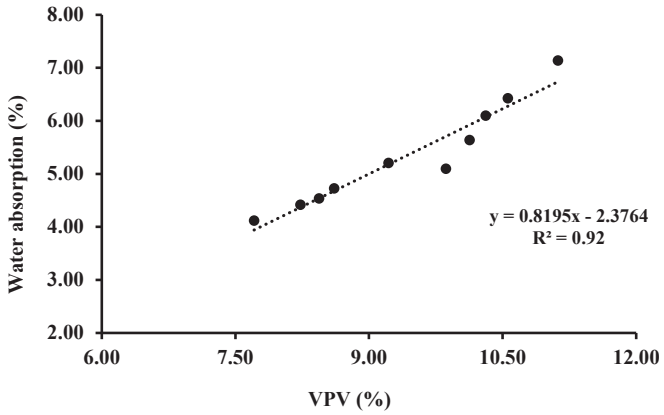

Fig. 8. Correlation between VPV and water absorption.

impact of fibers on minimizing water absorption and enhancing the density of concrete.

3.3. Mechanical properties

3.3.1. Compressive strength

Fig. 9**(a)** shows the compressive strengths of CAC composites made with different types and amounts of fibers (SF and PF) after 7 days of curing at 40 °C and 60 °C. For the control sample, compressive strength was recorded at 33.9 MPa and 26.8 MPa at 40 °C and 60 °C, respectively. The inclusion of SF significantly boosted the compressive strength at 40 °C, while the inclusion of PF resulted in a slight decrease compared to the control mix. Especially, the SF1 and SF2 mixes showed compressive strength increases of 5.0 % and 1.8 %, respectively, with values of 35.6 MPa of ITZ, polypropylene fibers specifically provide certain features, such as hydrophobicity, a lower modulus of elasticity, specific aspect ratios, and distinct surface morphologies. These characteristics jointly influence the ITZ, which in turn affects the compressive strength of the concrete [40]. SF demonstrated a more substantial effect on compressive strength improvement compared to PF. The superior performance of SF can be attributed to its higher strength, which enhances the efficiency of bridging macro-cracks, thus improving compressive strength. The best-performing mix was SF1, with compressive strengths of 35.6 MPa at 7 days and 34.4 MPa at 28 days under 40 °C curing conditions. This suggests a careful balance is required when considering higher fiber dosages, as seen in the optimal performance of SF1. Increased curing temperatures generally reduced the compressive strength of CAC specimens, with those cured at 60 °C showing the lowest strengths. This reduction is primarily due to the faster kinetics of metastable phase conversion at higher temperatures, as well as corresponding porosity changes [41]. Changes in the density of the hydrated phases lead to differences in compressive strengths. The hexagonal and 34.5 MPa. This increase can be attributed to SF's ability to impede microcrack formation and propagation, thereby enhancing the concrete's structural integrity [42,43]. The slight strength increases with 2 % SF compared to 1 % SF appears to be the result of the fibers dispersing less uniformly at higher doses. This is in line with what other research has found about traditional concrete [44]. Conversely, at 40 °C, PF1 and PF2 exhibited compressive strengths of 31.0 MPa and 29.0 MPa, respectively, denoting a minor decline from the control. Higher dosages of PF pose difficulties in maintaining the ideal compressive strength, indicating that a higher amount of PF may have a detrimental effect on the strength qualities of the matrix. At 60 °C, the enhancement in compressive strength was more pronounced for SF mixes. SF1 and SF2 demonstrated strength increases of 17.5 % and 11.2 %, respectively, over the control mix. PF1 showed a modest strength gain of 4.5 %, while PF2′s strength was 3.7 % lower than the control, likely due to fiber agglomeration at higher dosages.

Fig. 9**(b)** shows the compressive strengths at 28 days. The control mix presented 27.2 MPa and 23.4 MPa at 40 °C and 60 °C, correspondingly. The SF1 mix at 40 °C displayed a significant 26.5 % increase in compressive strength (34.4 MPa), indicating SF's positive impact on long-term strength development. In contrast, PF2 at 2 % dosage showed a notable reduction in strength (26.3 MPa). In addition, at 60 °C, all fiber-reinforced mixes demonstrated significant strength improvements. SF1 and SF2 had compressive strengths 30.3 % and 16.7 % higher than the control mix, respectively. PF1 and PF2 also showed higher strengths of 7.7 % and 1.7 %, respectively. Polypropylene fibers (PF) play a significant role in the development of an interfacial transition zone (ITZ) within concrete, which can have notable effects on its compressive strength. The unique properties of polypropylene fibers make their impact on the ITZ particularly significant [45]. Because of their hydrophobic nature, they repel water and, as a result, affect the hydration

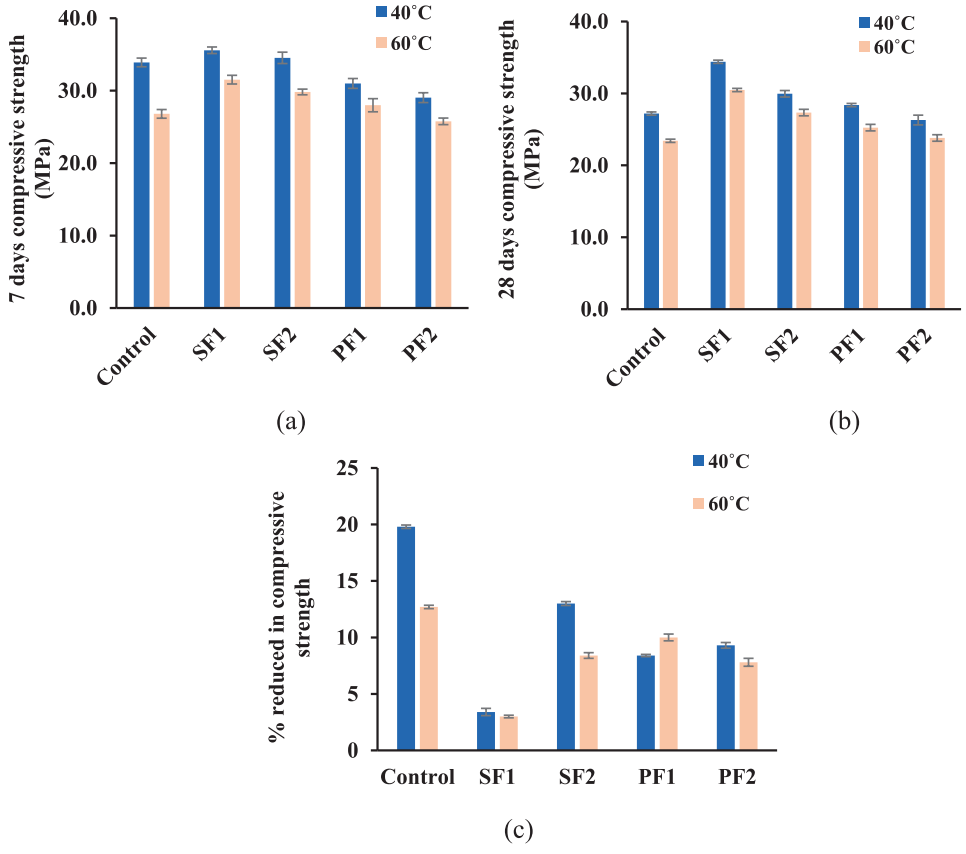

Fig. 9. Compressive strength analysis: (a) performance of fiber-reinforced mortar at 7 days, (b) performance at 28 days, and (c) percentage decrease in compressive strength from 7- to 28-day under elevated temperatures at 40 °C and 60 °C.

process in the cementitious matrix around them. The hydrophobic characteristic of a substance can cause alterations in the microstructure of the ITZ. Although all fibers contribute to the creation crystal forms of CAH_{10} and C_2AH_8 develop strength properties that are not present in the more compact cubic C_3AH_6 phase.

In the control sample, the complex process of CAC conversion is responsible for the observed decrease in compressive strength from 7 to 28 days at both curing temperatures (refer to Fig. 9**c**). The initial increase in strength detected after 7 days indicates the early process of hydration and chemical reactions occurring inside the combination. Over time, more water absorption and the creation of hydration products result in a reduction in compressive strength after 28 days. The decrease in strength, in comparison to OPC samples, is ascribed to the augmented porosity caused by the conversion process. As outlined in Eqs. (1) and (2), the transformation of CAH_{10} and C_2AH_8 into C_3AH_6 leads to the release of 60 % and 37.5 % of chemically bound water, respectively. This results in volume decreases of 53 % and 34 % in the hydration products, as stated in reference [41]. The notable alterations in volume have a role in the heightened porosity observed in CAC samples, which is associated with a decline in strength. OPC specimens increase in strength over time as a result of the hydration of C_2S and C_3S and the continuous creation of more CSH gel [41]. On the other hand, CAC specimens undergo a decrease in compressive strength owing to the conversion process. Nevertheless, the decrease is counteracted by the addition of fibers. The SF and PF mixes exhibited a range of percentage reductions in compressive strength, varying from 19.8 % to 3.4 % at 40 °C and from 12.7 % to 3 % at 60 °C. The occurrence of secondary porosity during the CAC conversion process is a significant concern, although the inclusion of fibers aids in reducing this impact. SF promote structural integrity by improving resistance to strength degradation and promoting long-term durability. Fiber reinforcing enhances the performance of CAC hydration products by increasing tensile strength and reducing fracture propagation. Lower dosages of PF lead to slower chemical reactions within the CAC matrix, thereby improving long-term compressive strength.

Hydration of the calcium aluminate phases in CAC produces hydrates like CAH_{10} and C_2AH_8. These hydrates increase the early-stage strength, but they cause it to drop during the CAC conversion process. When these hydrates change into stable phases like C_3AH_6, they change the material's density and strength, letting go of secondary water and creating new pores. This phenomenon is carried out by XRD and FESEM analyses, which reveal the development of crystalline phases and microstructural changes. The increased porosity facilitates chemical ingress, potentially causing corrosion in reinforced concrete with steel bars. Comprehending the formation of secondary water porosity and its effect on mechanical strength is crucial, since it contributes to the occurrence of building failures related to CAC. The integration of SF and PF in CAC mortar improves its mechanical properties and durability, reducing water absorption and porosity and contributing to the longevity and eco-friendliness of structures. These findings underscore the importance of fiber reinforcement in enhancing the performance of CAC composites under various curing conditions. It can be clearly seen that the current research data at 40 °C and 60 °C are similar to the previous research data at room temperature [7]. This shows that fiber reinforcement is a strong way to make CAC composites last longer in a variety of settings.

3.3.2. *Direct tensile strength*

The influence of fiber reinforcement was highlighted on the tensile strength of the CAC material, which was cured for 28 days at temperatures of 40 °C and 60 °C (Fig. 10). Initially, samples without fibers had a tensile strength of 2.9 MPa, serving as a baseline for comparison. The inclusion of SF and PF in the CAC mixture remarkably improved tensile strength. At 40 °C, incorporating 1 % and 2 % SF by volume led to increases in tensile strength of approximately 67 % and 48.3 %, respectively. This enhancement aligns with findings from previous research [7], which noted that SF can improve the tensile characteristics of

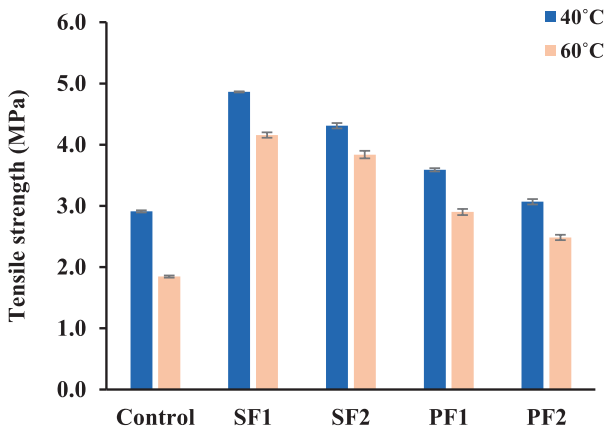

Fig. 10. Direct tensile strength outcomes.

concrete by inhibiting the initiation and propagation of cracks. Nonetheless, increasing the SF content beyond a certain point can lead to fiber agglomeration, thereby impairing effective fiber dispersion and crack bridging, ultimately reducing tensile strength. The results for PF mixtures at 40 °C were similarly noteworthy. The inclusion of 1 % and 2 % PF resulted in tensile strengths of 3.6 MPa and 3.1 MPa, respectively. These figures correspond to improvements of 24 % and 7 % compared to the control mix. Although there was a slight decline in tensile strength by 2 % with the increased PF content, the performance remained superior to that of the control. This observation is consistent with previous studies, which indicate that excessive amounts of PF can hinder fiber dispersion, thus diminishing the concrete's capacity to withstand external forces.

The specimens' performance at 60 °C yielded more convincing evidence. The control mix had a tensile strength of 1.8 MPa at this particular temperature. The SF1, SF2, PF1, and PF2 mixtures exhibited impressive tensile strengths of 4.2 MPa, 3.8 MPa, 2.9 MPa, and 2.5 MPa, respectively. The SF1, SF2, PF1, and PF2 mixtures were respectively 133 %, 111.1 %, 61.1 %, and 38.9 % greater than the control, as indicated by these data. The exceptional performance of SF can be attributed to its significantly higher tensile strength, which is approximately eight times greater than that of PF. This makes SF more efficient at minimizing the impact of large cracks in concrete.

In our prior study [7] conducted at room temperature, we observed comparable patterns. The tensile strengths for the control, SF1, SF2, PF1, and PF2 were measured at 2.5 MPa, 4.2 MPa, 3.9 MPa, 3.0 MPa, and 2.7 MPa, respectively. By comparing the results obtained at 40℃ and 60℃, it becomes evident that higher curing temperatures have a substantial impact on the tensile strength of CAC. The reason for this is the CAC conversion process, which enhances porosity while reducing mechanical strength. Fibers are essential in reducing these harmful consequences because they obstruct the spread of cracks and connecting spaces, thus maintaining the material's strength and stability.

Remarkably, the tensile strength of fiber-reinforced specimens regularly surpassed that of the control, despite the fact that higher curing temperatures typically decrease tensile strength by speeding up conversion and increasing porosity. Significantly, SF1 exhibited a tensile strength of 4.2 MPa at both room temperature and 60℃, showcasing the strong and durable performance of SF even in challenging environments. Conversely, mixtures reinforced with PF showed reduced tensile strengths at 60℃ compared to room temperature, suggesting that PF may be less efficient during curing at high temperatures. The tensile strength data highlight the crucial importance of fiber reinforcing, particularly SF, in enlightening the mechanical properties of CAC at different curing temperatures. The fibers' capacity to mitigate the adverse impacts of the conversion process underscores their essential role in preserving and enhancing the structural performance of CAC.

3.3.3. Flexural strength

The flexural strength values for all samples following a 28-day curing time at increased temperatures of 40 °C and 60 °C are displayed in Fig. 11. According to the information provided in Table 6, the CAC mortar reinforced with fibers showed significantly greater flexural strengths compared to the control mixture. The results confirm the findings of the tensile strength test, demonstrating that the flexural strength increases when up to 1 % fiber content is added. However, as the amount of fiber reached a certain threshold, the flexural strength declined. These data align with a previous research [2], which found that fiber-reinforced mortars have higher flexural strength compared to standard concrete mixes.

The flexural strength of the control mix was determined to be 7.6 MPa. However, the addition of 1 % SF at a temperature of 40 °C resulted in the highest recorded flexural strength of 9.7 MPa, which aligns with the published values for compressive and tensile strengths. Overall, the samples demonstrated an increase in volume and a little reduction in flexural strength when the fiber content exceeded 2 %. Nonetheless, the specimen with a 2 % SF volume still showed higher flexural strength when compared with the control mix. The addition of 1 % and 2 % SF to the specimens resulted in respective increases in the mortar's flexural strength of 27.6 % and 19.7 %, respectively. Similarly, the flexural strength of the PF mortar samples went up by about 15.8 % and 9.2 % when the PF level was 1 % and 2 %, respectively, compared to the control mixture. **Section 3.6**, based on a study of the fracture surface of mortar (Fig. 14**d**), explained this variance with the unequal distribution of PF fibers. Li et al. [42] had demonstrated through pullout tests and numerical simulations that the interaction between fibers and the matrix significantly influences the effectiveness of fiber reinforcement. PF fibers, particularly long ones, can negatively impact the mechanical properties of the matrix by adhering to each other during the mixing process. This agglomeration can increase the matrix's susceptibility to the formation of voids and cracks, thereby hindering the development of strength [43].

The performance of specimens at 60 °C provided additional compelling evidence. At this temperature, the flexural strength of the control mix reached 6.5 MPa. The flexural strengths of the SF1, SF2, PF1, and PF2 mixtures were 8.9 MPa, 8.3 MPa, 8.0 MPa, and 7.6 MPa, respectively, which were outstanding. The SF1, SF2, PF1, and PF2 mixes exhibited increases of 36.9 %, 27.7 %, 23.1 %, and 16.9 %, respectively, compared to the control, as seen by the provided data. The study [46] also found that high temperature curing conditions led to increased strength, which is consistent with the acquired results.

The markedly superior flexural strength of SF accounts for its outstanding performance. The current investigation's findings clearly show that the inclusion of PF has specific effects on concrete's flexural strength. Because PF had a lower tensile strength and elastic modulus than SF, its main function was to fill up micro-cracks with minimal effect on flexural strength. On the other hand, due to their greater ability to withstand stretching and their ability to resist deformation, SF had a considerable impact on the ability of concrete to withstand bending forces. In addition, these results demonstrate the complexity of the impact of higher curing temperatures on the CAC conversion process when compared to earlier research at ambient temperature. At 40 °C, there are certain advantages in terms of strength; however, at 60 °C, strength is typically diminished compared to both ambient and 40 °C conditions. The results unequivocally demonstrate that increased temperatures significantly affect the flexural strength of CAC mortar, in contrast to prior investigations conducted under normal ambient temperatures. The flexural strength of the fiber-reinforced specimens typically exhibited an increase when subjected to a temperature of 40 °C, as compared to the circumstances at room temperature. Nevertheless, when the temperature reaches 60 °C, there is a clear decrease in flexural strength for all combinations.

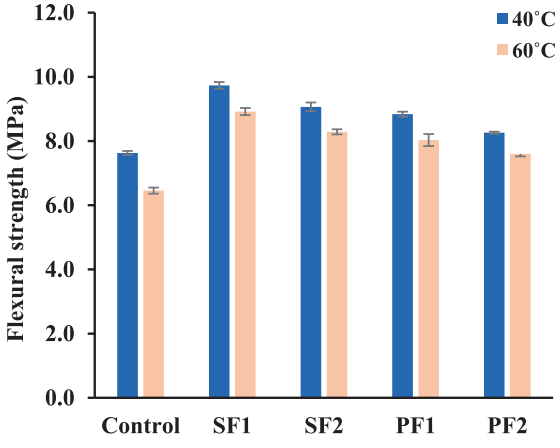

Fig. 11. Flexural strength results.

Table 6
Mechanical properties result for all specimens cured for 28 days at curing conditions of 40 °C and 60 °C.

Mix	Mechanical properties at 28 days (MPa)*					
	Compressive strength		Tensile strength		Flexural strength	
	40 °C	60 °C	40 °C	60 °C	40 °C	60 °C
Control	27.2 ± 0.23	23.4 ± 0.23	2.9 ± 0.02	1.8 ± 0.02	7.6 ± 0.06	6.5 ± 0.10
SF1	34.4 ± 0.23	30.5 ± 0.23	4.9 ± 0.01	4.2 ± 0.04	9.7 ± 0.10	8.9 ± 0.11
SF2	30.0 ± 0.45	27.3 ± 0.45	4.3 ± 0.04	3.8 ± 0.06	9.1 ± 0.14	8.3 ± 0.08
PF1	28.4 ± 0.23	25.2 ± 0.45	3.6 ± 0.03	2.9 ± 0.05	8.8 ± 0.08	8.0 ± 0.19
PF2	26.3 ± 0.68	23.8 ± 0.45	3.1 ± 0.04	2.5 ± 0.04	8.3 ± 0.03	7.6 ± 0.08

*Data show mean value ± standard deviation.

Unlike compressive strength, the presence of fibers has a significant impact on tensile and flexural strengths, resulting in a more pronounced effect. The reason for this disparity is that, when subjected to tension, the fibers' stress-transfer function starts earlier, resulting in crack formation with less energy compared to when subjected to compression [43]. The flexural strength test findings clearly indicate that the inclusion of fibers significantly improves the mortar's strength. However, an excessive amount of fiber content can negatively impact workability by causing fibers to clump together. This agglomeration hinders the mechanical bond between the cement paste and the fibers, leading to a decrease in flexural strength, especially noticeable in mixtures containing 2 % fibers. At the 2 % fiber content dosage, the concrete samples demonstrated a noticeable increase in volume alongside a decrease in flexural strength compared to those with a 1 % fiber dosage. The increase in volume at the 2 % dosage can be attributed to the higher fiber concentration, which increases the likelihood of fiber agglomeration within the matrix. This agglomeration introduces additional air voids and micro-pores, resulting in an overall expansion of the sample volume. In contrast, a 1 % fiber content allows for a more even dispersion within the matrix, minimizing air voids and better preserving matrix cohesion.

The decrease in flexural strength observed at the 2 % fiber dosage is likely due to the fiber clustering effect, which disrupts the uniform distribution of stress across the matrix. With increased fiber dosage, the agglomerated fibers create localized weaknesses, limiting effective load transfer and reducing the sample's resistance to bending stresses. At 1 %, the fibers remain sufficiently dispersed, enabling them to bridge microcracks and distribute loads more effectively, thereby enhancing flexural strength. Testing fiber contents between 1 % and 2 % could further illuminate the relationship between fiber dosage and mechanical properties, but the available data indicate that at 2 %, the concrete's mechanical integrity is compromised due to both increased volume and

reduced flexural strength relative to the 1 % dosage.

As the link between the fibers weakens, their capacity to span cracks decreases, leading to a decline in the flexural strength of the concrete. The flexural strength of the composites is less negatively impacted by CAC conversion hydration when fibers are included. The utilization of fibers also enhances flexural strength, similar to the reported improvement in compressive strength. Additionally, fibers play a crucial role in limiting microcrack propagation and preventing crack formation, thus enriching both flexural and compressive strength [44,45].

After examining the results of the flexural strength analysis, it becomes clear that the inclusion of fibers has a significant impact on both the ability of the mortar specimens to sustain loads and their tendency to develop cracks. The inclusion of fibers, specifically SF, results in a noticeable increase in flexural strength. Still, it is important to learn more about how this behavior happens, especially how the fibers and matrix interact and how that affects how cracks start and spread. According to the results, the specimens with SF exhibited higher flexural strength than the ones with PF. The variance can be ascribed to

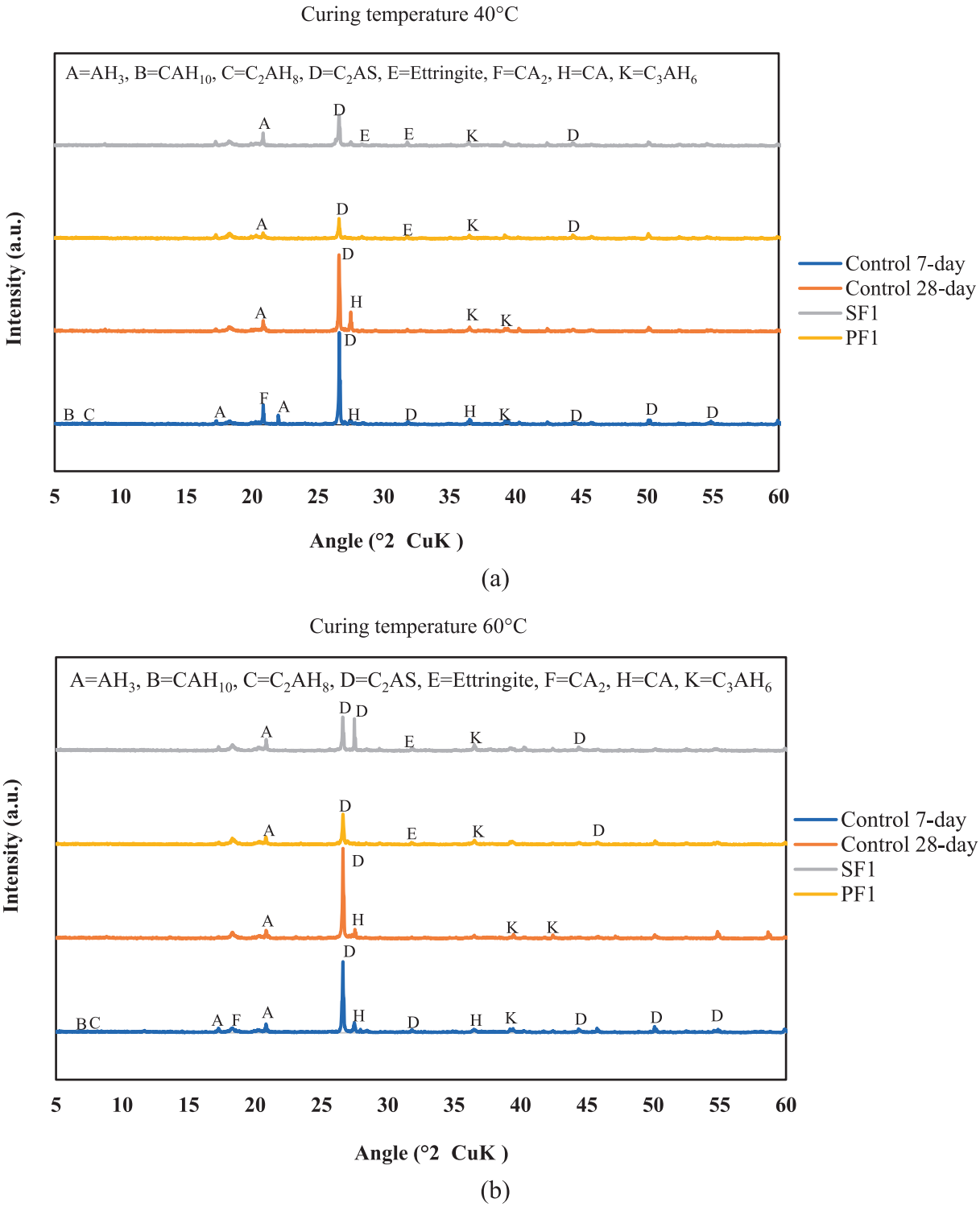

Fig. 12. XRD patterns for CAC systems containing fibers at elevated curing temperature: (a) 40 °C and (b) at 60 °C.

variations in the mechanical properties and fiber configuration inside the mortar substrate. SF is highly efficient at connecting small cracks and preventing crack spread, resulting in improved bending resistance and increased flexural strength. In addition, analyzing the fracture surface morphology (Fig. 14) offers vital understanding of the mechanisms that control the creation and spread of fractures in fiber-reinforced CAC concrete. In order to maximize flexural strength and reduce the chance of early cracking, it is crucial to comprehend these processes and optimize the number and influence of fibers.

Regarding the sensitivity of these parameters, the results indicate that fiber content and curing temperature have a significant impact on the mechanical properties of CAC composites. An increase in fiber dosage enhances tensile and flexural strengths but may reduce workability. Similarly, elevated curing temperatures accelerate early-age strength development; however, they can also induce microstructural changes that may affect long-term durability. These findings highlight the complex interactions between fiber reinforcement and CAC hydration at high temperatures, emphasizing the need for a balanced approach in material design.

To further optimize the interactions between fibers and CAC, several strategies could be explored. Surface modification of fibers, such as through chemical treatments or coatings, could improve the bonding between fibers and the CAC matrix, enhancing mechanical performance and reducing the impact of conversion effects. Additionally, fiber hybridization, combining different types of fibers (e.g., steel with synthetic or natural fibers), could leverage the unique benefits of each, improving flexural strength and crack resistance while mitigating temperature-induced expansion or shrinkage. Optimizing fiber dosage is also crucial, as the ideal fiber content—considering factors such as fiber length, aspect ratio, and distribution—can maximize the positive effects of reinforcement without compromising the material's workability. Fine-tuning curing conditions, including temperature and humidity, could further enhance fiber performance and reduce thermal stresses during the conversion process. Finally, the incorporation of nanomaterials, such as graphene or carbon nanotubes [47–50], could improve the interfacial bond between fibers and the matrix, enhancing the material's resistance to thermal degradation and increasing overall durability. These strategies could unlock more resilient and sustainable fiber-reinforced CAC materials, particularly in environments with extreme temperature fluctuations.

3.4. XRD analysis

The findings of the XRD studies of the hydrated materials are shown in Fig. 12**(a) and (b)**. The dataset comprises control samples that were evaluated at 7-day and 28-day intervals while being subjected to elevated temperatures of 40 °C and 60 °C. In addition, SF1 and PF1 samples were collected every 28 days. The CAC method easily detected typical CAC hydrates such as CAH_{10}, C_2AH_8, and C_3AH_6, along with the crystalline gibbsite (AH_3). The control samples, which did not include fibers, exhibited unreacted clinker phases consisting of monocalcium aluminate. The cubic phase C_3AH_6 was found, and its interaction with C_3AH_6 to make calcium aluminum silicate hydrate was also noted [18]. This was especially clear in the XRD tests done on the control sample that had been developed at 40 °C for 7 days. Minor amounts of AH_3 and a new hydrated calcium aluminosilicate crystalline phase were detected in the CAC composites. The cubic phase (C_3AH_6) appeared more prominently in the control sample cured at 60 °C for 28 days. These X-ray results align with the TGA analyses, which did not clearly identify crystalline gibbsite or hexagonal hydrates in the samples. The 28-day-cured control sample notably marked the presence of the cubic phase (C_3AH_6). These findings are in line with earlier research [7], which showed that CAC-mixed cements go through normal hydration processes and form cubic or hexagonal hydrates. The XRD spectra of these hydrated materials containing fibers, cured at 40 °C, were similar to those cured at 60 °C.

These findings offer valuable understanding of how the inclusion of fiber impacts the chemical composition and water transport dynamics in the CAC matrix. This aids in gaining a deeper comprehension of the fluctuations in compressive strength that arise when subjected to elevated temperatures. The addition of fibers leads to significant changes in the XRD patterns, suggesting modifications in hydration products and crystalline phases. Initially, in the presence of a little amount of water, the XRD pattern exhibits diffraction peaks corresponding to unhydrated forms of CA, CA_2, and C_2AS. Following a 28-day hydration interval, the peaks associated with unhydrated CA and CA_2 exhibit a rapid reduction. However, the presence of fibers accelerates the hydration process of CA, leading to the formation of main hydration products including CAH_{10}, AH_3, and C_2AH_8. The AH_3 diffraction peak displays a significant increase in intensity, influenced by several factors including as temperature, humidity, and curing duration. Elevated temperatures, specifically 60 °C, expedite the process of hydration reactions, resulting in augmented formation of AH_3 and amplified peak intensities in the XRD patterns [41]. In contrast, lower temperatures, such as around 20 °C, decelerate the hydration process, leading to a less significant increase in AH_3 intensity [7]. Variations in humidity can also impact the quantity of water accessible for hydration activities, therefore influencing the formation of AH_3.

Furthermore, extended curing times and elevated temperatures allow for more extensive hydration, leading to further development of AH_3 and C_3AH_6 [6,41]. At the same time, C_2AH_8 diffraction peaks decrease over the 28-day curing period, as well as temperature. Remarkably, there was no indication of stratlingite formation in the XRD analysis. The inclusion of fibers can modify the rate of hydration, thereby changing the strength and position of the diffraction peaks related to these hydration products. In addition, the inclusion of fibers can modify the microstructural characteristics of the hydrated materials, potentially causing alterations in nucleation and crystal growth mechanisms of crystal phases (refer to Fig. 14) [51].

3.5. Thermogravimetric analysis

The TGA curves of fibers-reinforced CAC composites, cured at temperatures of 40 °C and 60 °C, are plotted in Fig. 13**(a) and 12(b)**, respectively. In addition, a water-hydrated CAC system that underwent curing at a temperature of 40 °C, the TGA curve exhibited an early peak at approximately 130 °C, which was attributed to the dehydration of CAH and alumina gel [52]. This peak became more pronounced as the curing period rose. The second peak, which occurred between 100 °C and 160 °C, represents the dehydration of CAH_{10} and C_2AH_8 [53]. This peak reached its highest point after 28 days of curing but was then reduced. The bands seen between 140 °C and 200 °C, which became more intense as the curing time and temperature increased, are associated with the removal of water from carboaluminate phases and subsequent dehydration of C_2AH_8. This suggests that the conversion process occurred at a temperature of 60 °C. Furthermore, the strength of the signal associated with the dehydration of gibbsite (AH_3) between 210 °C and 300 °C [7] exhibited an upward trend as the duration of curing increased. The signal linked to C_3AH_6 cubic compounds appeared between 240 °C and 370 °C [53] after a curing period of 7 days and increased in intensity until 28 days.

Total weight loss generally increased with fibers added and curing time progressed. The total weight loss values ranged from 6.9–9.9 wt% in the fibers-reinforced CAC composites system at 40 °C and up to 7.8–11.0 wt% in those elevated temperature for 60 °C. These results were slightly higher in the fiber-reinforced CAC composites system cured at 60 °C (7.8 wt% in control sample 7-day, 11.0 % in control sample 28-day, 7.9 % in SF1, and 9.3 % in PF1), reflecting faster reaction progress at the higher temperature. These results exhibit a strong correlation with the observed development of compressive strength. Moreover, the quantity of C_3AH_6 is recognized as a crucial determinant in the transformation process associated with hydration, and it may be

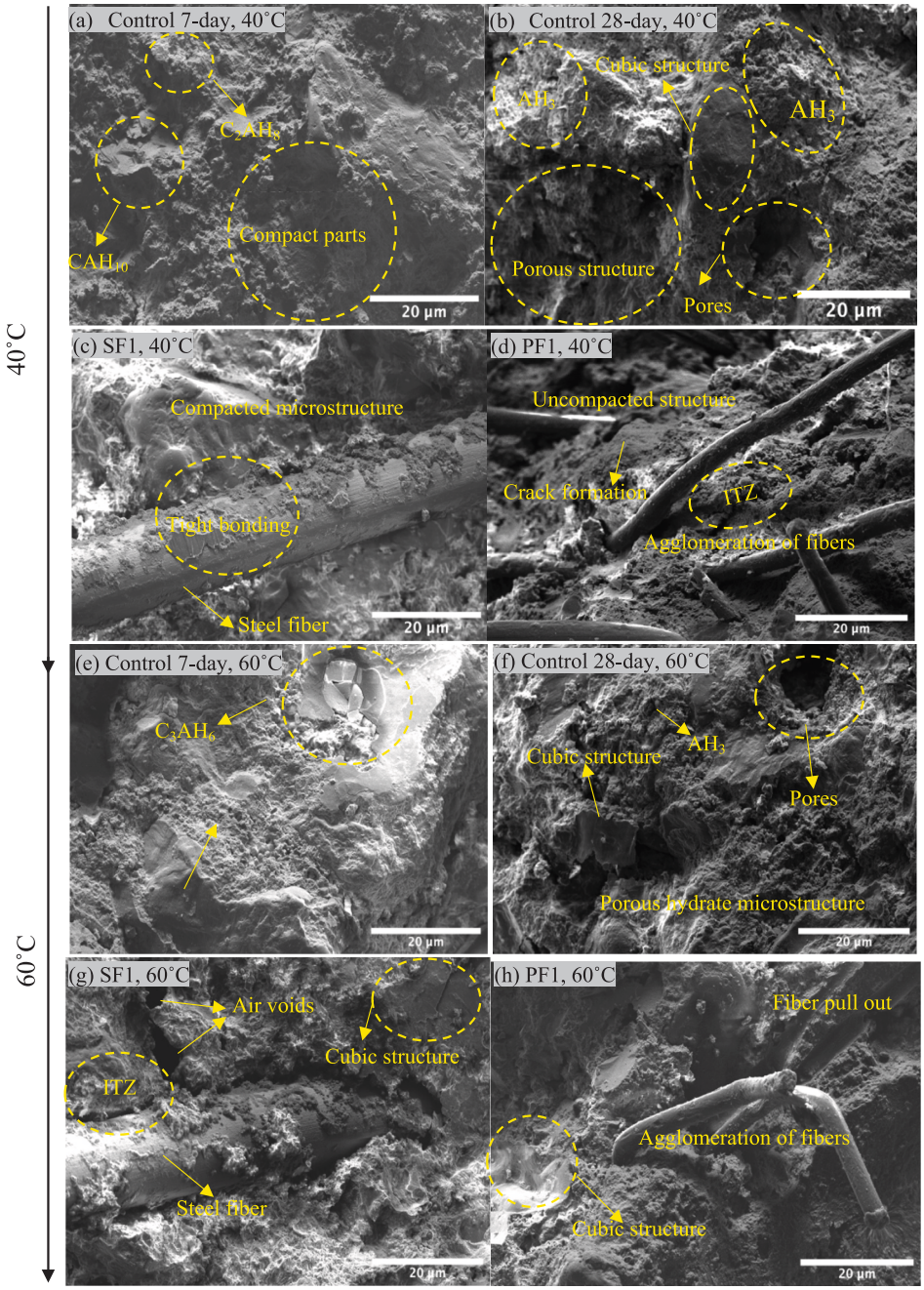

Fig. 13. Microstructure for CAC systems of different types of fibers under 40 °C and 60 °C (FESEM image captured at a magnification of 500x).

quantified using TGA. During the thermal disintegration of hardened CAC, different aluminate hydrates undergo decomposition, resulting in the release of chemically bound water, as described in **Eqs. (3)–(6)**. This work highlights that the release of confined water from C_3AH_6 takes place at around 300 °C. The results align with previously recorded breakdown temperatures for CAC hydrates [54,55].

$$CAH_{10} \rightarrow CaAl_2O_4 + 10H_2O\ (100 - 160\ ^\circ C) \quad (3)$$

$$C_2AH_8 \rightarrow Ca_2Al_2O_5 + 8H_2O\ (140 - 200\ ^\circ C) \quad (4)$$

$$AH_3\ Al_2O_3 + 3H_2O\ (210 - 300\ ^\circ C) \quad (5)$$

$$C_3AH_6\ Ca_3Al_2O_6 + 6H_2O \rightarrow (240 - 370\ ^\circ C) \quad (6)$$

The analysis confirmed the existence of hydrate phases CAH_{10} and C_3AH_6, despite the absence of C_2AH_8 and AH_3 in the samples. At a temperature of 60 °C, a substantial proportion of C_2AH_8 underwent a transformation into AH_3 and C_3AH_6. This transformation is caused by the conversion of the metastable hexagonal CAH_{10} phase into the cubic C_3AH_6 phase. Eq. (7) [6] was utilized to determine the quantity of C_3AH_6 in the fiber-reinforced CAC system.

$$C_3AH_{6,measured} = WL_{C_3AH_6} \times \frac{m_{C_3AH_6}}{6 \times m_{H_2O}} \quad (7)$$

The term "$C_3AH_{6,measured}$" refers to the quantified quantity of C_3AH_6 present in the mixture, expressed as a percentage. The variable WL_{C3AH6} represents the percentage of weight lost as a result of water evaporation between the temperatures of 240 to 370 °C [55]. Here, m_{C3AH6} and m_{H2O} indicate the molar masses of C_3AH_6 (378 g/mol) and water (18 g/mol), respectively.

Table 7 presents the calculated proportions of the transformed cubic C_3AH_6 phase in fiber-reinforced CAC cured at 40 °C and 60 °C. The final

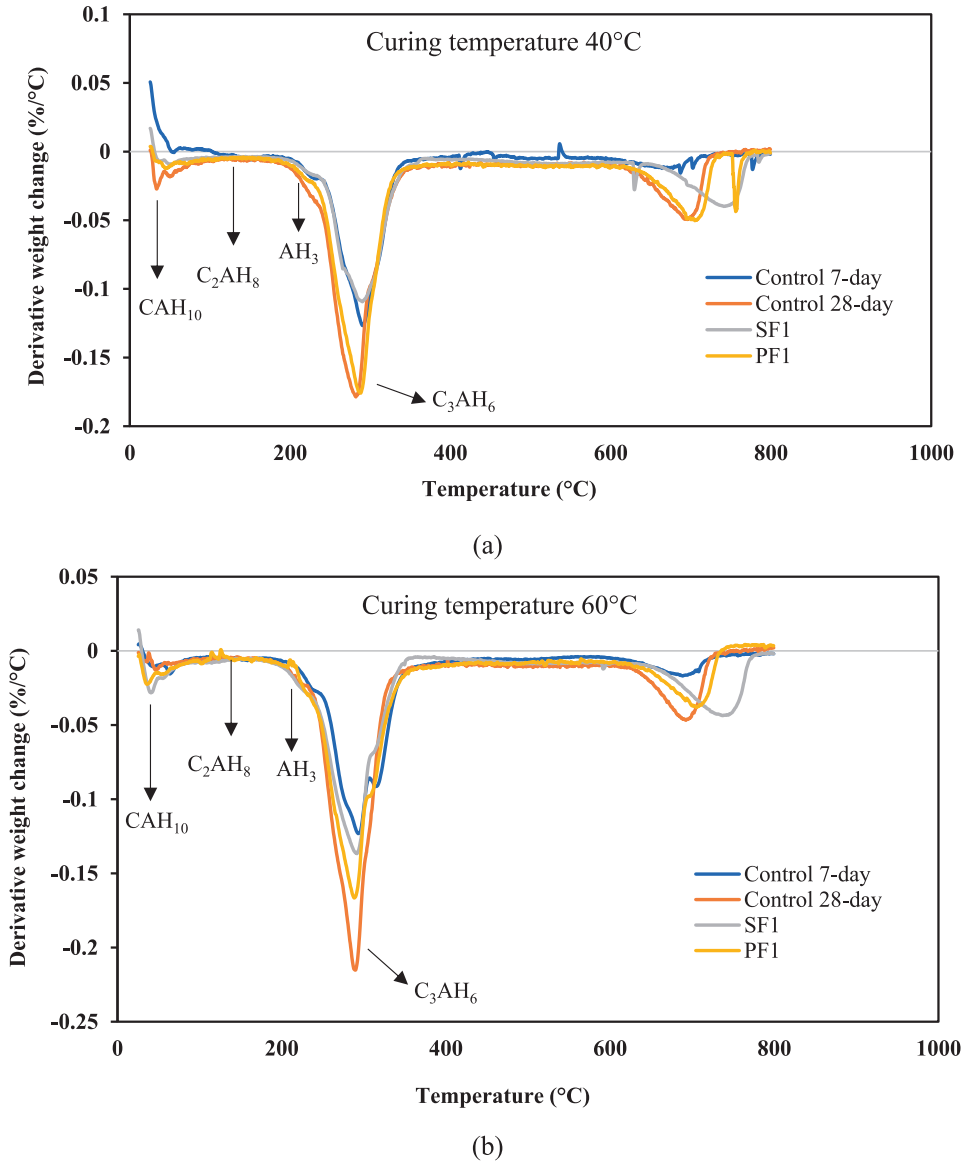

Fig. 14. The differential thermogravimetry curve of CAC composites incorporating fibers: (a) 40 °C and (b) at 60 °C.

Table 7
Quantitative analysis of C_3AH_6 phase content.

Mix	C_3AH_6 phase content %		$\Delta_{60-40}C_3AH_6$ (%)
	40 °C	60 °C	
Control 7-day	24.2	27.5	13.6
Control 28-day	34.8	38.4	10.3
SF1	24.3	27.8	14.4
PF1	32.8	33.1	0.9

column of Table 7 highlights the percentage difference in C_3AH_6 content between samples cured at these two temperatures. The TGA results allow us to draw the following conclusions:

(1) The fibers in the mixture affected how much CAC was converted;

(2) Curing CAC samples at ambient temperature (20 °C) in the previous study [7] made the conversion much less influential to the compressive strength (only 2 % for SF);

(3) Increasing the curing temperature from 40–60 °C made the conversion of the CAC samples even less influential;

(4) At 40 °C, the formation of C_3AH_6 led to a lower degree of conversion, but at 60 °C, it led to a higher degree of conversion and the formation of more C_3AH_6.

In addition, the findings suggest that the fiber incorporation in CAC composites, particularly in blends SF1 and PF1, led to a decrease in the formation of C_3AH_6. The XRD data verify this discovery, indicating that the inclusion of fibers in CAC diminishes the synthesis of C_3AH_6, resulting in a reduced quantity compared to the control sample after curing for 28 days. In addition, the proportion of the C_3AH_6 phase in all samples was much decreased compared with the samples at 60 °C. The XRD results were consistent with the presence of the C_3AH_6 phase at 300 °C in the activated pastes including fibers in CAC cured at 40 °C and 60 °C. The strength of this effect increased with longer curing time and higher temperature. While there was a little variation observed in the TGA curve for the fiber-reinforced CAC composites cured at 40 °C, the XRD investigations were unable to clearly identify the cubic phase in the samples. The reduction in C_3AH_6 production, as detected by TGA and XRD studies, can be linked to structural alterations discovered by FESEM (refer to Fig. 14). This contributes to a comprehensive understanding of how fiber reinforcement affects the CAC conversion process.

3.6. FESEM analysis

Fig. 14 depicts the microstructural characteristics of several mortar mixtures containing SF and PF cured at two elevated temperatures. Fig. 14**(a)–(d)** show the formation of plate- and sheet-shaped crystals of CAH_{10} and C_2AH_8 after curing at 40 °C. As these crystals accumulate and overlap, AH_3 attaches to their surfaces. CAH_{10} and C_2AH_8 crystals are growing, such as larger sizes and denser arrangements, which make specimens last longer. These observations emphasize the importance of paste hydration, as well as the distribution and shape of hydration products, in influencing the material's strength. The presence of these crystal morphologies impacts the composite's strength and durability, as CAH_{10} and C_2AH_8 are known to provide a stable matrix structure that supports the load-bearing capacity of the composite. Specifically, the plate-like CAH_{10} crystals contribute to densification, enhancing compressive strength by reducing porosity within the matrix. Similarly, the sheet-like morphology of C_2AH_8 plays a role in increasing the matrix's binding capability, which reinforces the structural integrity of the composite. Additionally, the inclusion of fibers within the CAC matrix not only provides reinforcement but also helps to bridge cracks, which limits crack propagation and enhances toughness. The interaction between these fibrous materials and the hydrates contributes to improved load distribution and energy absorption, resulting in better mechanical performance under stress. At 40 °C, the compressive strength of the control mix decreased by approximately 20 % between the 7- and 28-day, as illustrated in Fig. 9**(b)**. This occurs because AH_3 is forming and there is a needle-shaped microstructure, which is typical of the unstable phase of CAH_{10}. The phase change from CAH_{10} to C_3AH_6 is responsible for the drop in compressive strength. Nevertheless, the presence of a more compact microstructure at a temperature of 40 °C corresponds to the obtained compressive strength outcomes. Fig. 14**(e)–(h)** show distinct pores in the CAC composites from samples subjected to a temperature of 60 °C. This phenomenon can be attributed to conversion hydration, resulting in a structure that is highly porous. Under elevated temperatures, the control sample exhibits an increase in both the size and number of pores at 28 days compared to 7 days. This leads to a deterioration of CAC's mechanical properties.

Nevertheless, fibers are added to the accomplished concrete to improve its density and refine its pores. The microstructural morphology is more finely detailed in the SF1 and PF1 mixes, as illustrated in Fig. 14**(c) and (d)**. The absence of CAH_{10} is the reason behind this (Fig. 14**b**). The control sample's compressive strength decreased by 19.8 % after 28 days at 40 °C, in line with Fig. 9**(c)**'s findings (approximately 3.4 % for SF1 and 8.4 % for PF1). The control sample's compressive strength decreased by 12.7 % after 28 days at a temperature of 60 °C, mirroring the decrease in Fig. 9**(c)**. The compressive strength of SF1 decreased by approximately 3.0 %, while the compressive strength of PF1 decreased by 10 %. These findings indicate that incorporating fibers into the CAC system typically leads to favorable results by reducing the conversion process. Fig. 9**(a) and (b)** demonstrate that the fibers, particularly SF1 and PF1, lead to a 26.5 % and 4.4 % increase in 28-day compressive strength at 40 °C and a 30.0 % and 7.7 % increase at 60 °C, respectively.

Polypropylene fibers (PF), due to their hydrophobic nature, significantly influence the microstructure of the Interfacial Transition Zone (ITZ) in concrete. The hydrophobicity of PF fibers reduces the absorption of water at the ITZ, which can help limit the formation of capillary pores and prevent water-induced weaknesses in the microstructure. This results in a more stable and durable ITZ, enhancing the overall integrity of the concrete. Additionally, the reduced moisture availability may alter the hydration process, leading to a denser ITZ microstructure, which can improve the bonding between the fiber and cement paste, despite the hydrophobic nature of the fibers. The presence of PF also helps in reducing the formation of microcracks, thereby improving the concrete's resistance to shrinkage, cracking, and chemical attacks. In essence, the hydrophobicity of PF contributes to enhancing the durability and mechanical properties of concrete by influencing the ITZ, ultimately resulting in better overall concrete performance. SF is recognized as a potent addition for reducing the conversion process, resulting in increased compressive strength at both 40 °C and 60 °C. The addition of chemical and mineral additives can alter the phase conversion of CAC [5,56]. However, including fibers in CAC mixes appears to be the most effective method for halting the conversion process, even under high-temperature curing conditions. As a result, the researchers recognize this innovative composite material as an eco-friendly, rapidly solidifying, and highly efficient type of concrete. It should be also noted that the CAC containing fibers is also generally used in special applications such as 3D printing concrete [57–61] for ameliorating their setting behavior and extrudability performance. Nonetheless, this area is not yet explored regarding the conversion of CAC.

4. Conclusions

This study investigates the influence of reinforcing fibers on CAC composites exposed to elevated curing temperatures. The findings highlight that the addition of SF and PF significantly enhances mechanical properties such as compressive, tensile, and flexural strengths. Notably, SF demonstrates superior efficacy at 40 °C, while its performance diminishes at 60 °C due to accelerated phase transformations in the CAC matrix. These insights contribute to optimizing fiber-reinforced CAC composites for sustainable and resilient construction applications.

1) The inclusion of fibers significantly reduced CAC mortar workability. SF led to a 14–17 % reduction, while PF caused a more pronounced 53–71 % decrease, depending on fiber dosage. Despite this, all mixtures maintained sufficient workability for practical applications, emphasizing the trade-off between fiber reinforcement and ease of handling.
2) Fiber reinforcement improved durability by reducing VPV and water absorption. SF exhibited greater effectiveness than PF in enhancing density and decreasing porosity, particularly at elevated curing temperatures.
3) The mechanical strength of CAC mortar improved significantly with SF, particularly at 40 °C. PF showed moderate improvements at 40 °C but exhibited reduced effectiveness at higher temperatures due to the conversion process. SF1 was notably more effective than PF1 in strengthening CAC mortar.
4) XRD analysis revealed that fiber reinforcement influenced crystalline phase formation, particularly C_3AH_6. Changes in diffraction peaks for CAH_{10}, AH_3, and C_2AH_8 were observed, with increased C_3AH_6 formation at 60 °C.
5) TGA analysis confirmed that higher curing temperatures (60 °C) accelerated the conversion of C_2AH_8 and AH_3 into C_3AH_6. SF mitigated C_3AH_6 development better than PF, contributing to enhanced strength and durability.
6) FESEM analysis demonstrated that fibers improved microstructural refinement, reduced pore sizes, and delayed phase conversion, leading to improved mechanical performance and resilience against harsh environmental conditions.

Despite the valuable insights gained, this study has certain limitations. It primarily focuses on synthetic fibers (SF and PF), and future research should explore eco-friendly alternatives such as natural or recycled fibers to enhance sustainability. Additionally, the long-term durability and performance of fiber-reinforced CAC composites in real-world conditions require further investigation, particularly their resistance to environmental factors such as freeze–thaw cycles and chemical degradation. Another key area for future exploration is the interplay between fiber reinforcement and low-carbon binders, such as geopolymer or fly ash-based cements, to develop more sustainable cementitious materials. Furthermore, advanced computational modeling and machine learning approaches could be leveraged to predict material

behavior, optimize mix designs, and refine performance assessments with greater precision, ultimately reducing the need for extensive experimental trials.

This study contributes to the broader field of construction materials by providing a detailed assessment of fiber-reinforced CAC composites. The findings demonstrate that fiber reinforcement can enhance durability and performance, potentially reducing reliance on energy-intensive Portland cement. These insights support the development of more resilient and sustainable building materials, paving the way for further innovation in alternative cement technologies.

CRediT authorship contribution statement

Thwe Thwe Win: Conceptualization, Methodology, Formal analysis, Writing – original draft, Investigation, Data curation. **Yiwei Weng:** Validation, Writing – review & editing. **Lapyote Prasittisopin:** Funding acquisition, Supervision, Writing – review & editing, Project administration, Conceptualization, Resources.

Declaration of competing interest

The authors declare that they have no known competing financial interests or personal relationships that could have appeared to influence the work reported in this paper.

References

[1] Abolhasani A, Shakouri M, Dehestani M, Samali B, Banihashemi S. A comprehensive evaluation of fracture toughness, fracture energy, flexural strength and microstructure of calcium aluminate cement concrete exposed to high temperatures. Eng Fract Mech 2022;261:108221. https://doi.org/10.1016/j.engfracmech.2021.108221.

[2] Afroughsabet V, Ozbakkaloglu T. Mechanical and durability properties of high-strength concrete containing steel and polypropylene fibers. Constr Build Mater 2015;94:73–82. https://doi.org/10.1016/j.conbuildmat.2015.06.051.

[3] Sharp J, Lawrence C, Yang R. Calcium sulfoaluminate cements—low-energy cements, special cements or what? Adv Cem Res 1999;11(1):3–13. https://doi.org/10.1680/adcr.1999.11.1.3.

[4] Juenger MCG, Winnefeld F, Provis JL, Ideker JH. Advances in alternative cementitious binders. Cem Concr Res 2011;41(12):1232–43. https://doi.org/10.1016/j.cemconres.2010.11.012.

[5] Win TT, Panwisawas C, Jongvivatsakul P, Pansuk W, Prasittisopin L. Effects of fly ash composition to mitigate conversion of calcium aluminate cement composites. Buildings 2023;13(10):2453. https://doi.org/10.3390/buildings13102453.

[6] Win TT, Prasittisopin L, Jongvivatsakul P, Likitlersuang S. Investigating the synergistic effect of graphene nanoplatelets and fly ash on the mechanical properties and microstructure of calcium aluminate cement composites. J Build Eng 2023;78:107710. https://doi.org/10.1016/j.jobe.2023.107710.

[7] Win TT, Prasittisopin L, Jongvivatsakul P, Likitlersuang S. Investigating the role of steel and polypropylene fibers for enhancing mechanical properties and microstructural performance in mitigating conversion effects in calcium aluminate cement. Constr Build Mater 2024;430:136515. https://doi.org/10.1016/j.conbuildmat.2024.136515.

[8] Hidalgo A, García J, Alonso M, Fernández L, Andrade C. Microstructure development in mixes of calcium aluminate cement with silica fume or fly ash. J Therm Anal Calorim 2009;96(2):335–45. https://doi.org/10.1007/s10973-007-8439-3.

[9] Revay M, Wagner Z. Determination of the expected decrease in strength of high alumina cement concrete by derivatography. Thermochim Acta 1979;31(3):365–74. https://doi.org/10.1016/0040-6031(79)80051-9.

[10] Ahmed A, Abubakr P, Salih Mohammed A. Efficient models to evaluate the effect of C3S, C2S, C3A, and C4AF contents on the long-term compressive strength of cement paste. Structures 2023;47:1459–75. https://doi.org/10.1016/j.istruc.2022.11.114.

[11] Ahmed W, Lim CW. Production of sustainable and structural fiber reinforced recycled aggregate concrete with improved fracture properties: a review. J Clean Prod 2021;279:123832. https://doi.org/10.1016/j.jclepro.2020.123832.

[12] Miah MJ, Pei J, Kim H, Sharma R, Jang JG, Ahn J. Property assessment of an eco-friendly mortar reinforced with recycled mask fiber derived from COVID-19 single-use face masks. J Build Eng 2023;66:105885. https://doi.org/10.1016/j.jobe.2023.105885.

[13] Prasittisopin L, Ferdous W, Kamchoom V. Microplastics in construction and built environment. Dev Built Environ 2023;15:100188. https://doi.org/10.1016/j.dibe.2023.100188.

[14] Hussain Z, Pu Z, Hussain A, Ahmed S, Shah AU, Ali A, et al. Effect of fiber dosage on water permeability using a newly designed apparatus and crack monitoring of steel fiber–reinforced concrete under direct tensile loading. Struct Health Monit 2022;21(5):2083–96. https://doi.org/10.1177/14759217211052855.

[15] Pachideh G, Gholhaki M. An experimental study on the effects of adding steel and polypropylene fibers to concrete on its resistance after different temperatures. J Test Eval 2019;47(2):1606–20. https://doi.org/10.1520/JTE20170145.

[16] Pachideh G, Gholhaki M. An experimental investigation into effect of temperature rise on mechanical and visual characteristics of concrete containing recycled metal spring. Struct Concr 2021;22(1):550–65. https://doi.org/10.1002/suco.201900274.

[17] Pachideh G, Gholhaki M, Moshtagh A. Performance of concrete containing recycled springs in post-fire conditions. Proc Instit Civil Eng-Struct Build 2020;173(1):3–16. https://doi.org/10.1680/jstbu.18.00042.

[18] Gholhaki M, Pachideh G, Rezayfar O. An experimental study on mechanical properties of concrete containing steel and polypropylene fibers at high temperatures. J Struct Constr Eng 2017;4(3):167–79. https://doi.org/10.22065/jsce.2017.77392.1072.

[19] Al-Sebai H, Al-Sadoon ZA, Altoubat S, Maalej M. Constitutive relations for modelling macro synthetic fiber reinforced concrete. Civil Eng J 2024;10(6):1806–27. https://doi.org/10.28991/CEJ-2024-010-06-06.

[20] Miftakhov E, Mustafina S, Kashnikova A, Akimov A. Development of a cloud service for comprehensive research of polymer synthesis processes. Emerg Sci J 2024;8(6):2539–53. https://doi.org/10.28991/ESJ-2024-08-06-023.

[21] Nassif N, Junaid MT, Maalej M, Altoubat S, Barakat SA. Durability of fiber-reinforced polymer (FRP) bars: progress, innovations and challenges based on bibliometric analysis. Civil Eng J 2024;10:136–73. https://doi.org/10.28991/CEJ-SP2024-010-09.

[22] ASTM C33-18. Standard Specification for Concrete Aggregates. West Conshohocken: American Society of Testing Materials; 2018.

[23] ASTM C109/C109M-16. Standard Test Method for Compressive Strength of Hydraulic Cement Mortars (using 2-in. or [50-mm] Cube Specimens). West Conshohocken: American Society of Testing Materials; 2016.

[24] ASTM C642-21. Standard Test Method for Density, Absorption, and Voids in Hardened Concrete. West Conshohocken: American Society of Testing Materials; 2021.

[25] Monaco M, Aurilio M, Tafuro A, Guadagnuolo M. Sustainable mortars for application in the cultural heritage field. Materials 2021;14(3):598. https://doi.org/10.3390/ma14030598.

[26] ASTM C348-21. Standard Test Method for Flexural Strength of Hydraulic-Cement Mortars. West Conshohocken: American Society of Testing Materials; 2021.

[27] ASTM C305-20. Standard practice for mechanical mixing of hydraulic cement pastes and mortars of plastic consistency. West Conshohocken: American Society of Testing Materials; 2020.

[28] Raj A, Yamkasikorn P, Wangtawesap R, Win TT, Ngamkhanong C, Jongvivatsakul P, et al. Effect of Graphene Quantum Dots (GQDs) on the mechanical, dynamic, and durability properties of concrete. Constr Build Mater 2024;441:137597. https://doi.org/10.1016/j.conbuildmat.2024.137597.

[29] ASTM C1437-20. Standard Test Method for Flow of Hydraulic Cement Mortar,. West Conshohocken: American Society of Testing Materials; 2020.

[30] ASTM C511-21. Standard specification for mixing rooms, moist cabinets, moist rooms, and water storage tanks used in the testing of hydraulic cements and concretes. West Conshohocken: American Society of Testing Materials; 2021.

[31] ASTM C305-20. Standard Practice for Mechanical Mixing of Hydraulic Cement Pastes and Mortars of Plastic Consistency. West Conshohocken: American Society of Testing Materials; 2020.

[32] Thwe Win T, Jongvivatsakul P, Jirawattanasomkul T, Prasittisopin L, Likitlersuang S. Use of polypropylene fibers extracted from recycled surgical face masks in cement mortar. Constr Build Mater 2023;391:131845. https://doi.org/10.1016/j.conbuildmat.2023.131845.

[33] Nuaklong P, Chittanurak J, Jongvivatsakul P, Pansuk W, Lenwari A, Likitlersuang S. Effect of hybrid polypropylene-steel fibres on strength characteristics of UHPFRC. Adv Concr Constr 2020;10(1):1. https://doi.org/10.12989/acc.2020.10.1.001.

[34] Bensted J. Calcium aluminate cements. Struct Performance Cem 2002;2:114–38.

[35] Sun Z, Xu Q. Microscopic, physical and mechanical analysis of polypropylene fiber reinforced concrete. Mater Sci Eng A 2009;527(1):198–204. https://doi.org/10.1016/j.msea.2009.07.056.

[36] Zaid O, Ahmad J, Siddique MS, Aslam F. Effect of incorporation of rice husk ash instead of cement on the performance of steel fibers reinforced concrete. Front Mater 2021;8:665625. https://doi.org/10.3389/fmats.2021.665625.

[37] Ahmad J, Manan A, Ali A, Khan MW, Asim M, Zaid O. A study on mechanical and durability aspects of concrete modified with steel fibers (SFs). Civ Eng Archit 2020;8:814–23. https://doi.org/10.13189/cea.2020.080508.

[38] Kaplan G, Bayraktar OY, Gholampour A, Gencel O, Koksal F, Ozbakkaloglu T. Mechanical and durability properties of steel fiber-reinforced concrete containing coarse recycled concrete aggregate. Struct Concr 2021;22(5):2791–812. https://doi.org/10.1002/suco.202100028.

[39] Placino P, Rugkhapan NT. Making visible concrete's shadow places: Mixing environmental concerns and social inequalities into building materials. Environ Urbanizat 2024;36(1):195–213. https://doi.org/10.1177/09562478231214140.

[40] ASTM C469/C469M-22, Standard Test Method for Static Modulus of Elasticity and Poisson's Ratio of Concrete in Compression, American Society of Testing Materials, West Conshohocken. 2022.

[41] Ahmed AA, Shakouri M, Trejo D, Pavan Vaddey N. Effect of curing temperature and water-to-cement ratio on corrosion of steel in calcium aluminate cement concrete. Constr Build Mater 2022;350:128875. https://doi.org/10.1016/j.conbuildmat.2022.128875.

[42] Li H, Liebscher M, Ly KH, Ly PV, Köberle T, Yang J, et al. Effect of electrophoretic deposition of micro-quartz on the microstructural and mechanical properties of

carbon fibers and their bond performance toward cement. J Mater Sci 2022;57(48):21885–900. https://doi.org/10.1007/s10853-022-07989-w.
[43] Li H, Yang J, Wang L, Li L, Xia Y, Köberle T, et al. Multiscale assessment of performance of limestone calcined clay cement (LC3) reinforced with virgin and recycled carbon fibers. Constr Build Mater 2023;406:133228. https://doi.org/10.1016/j.conbuildmat.2023.133228.
[44] Wu Z, Shi C, He W, Wu L. Effects of steel fiber content and shape on mechanical properties of ultra high performance concrete. Constr Build Mater 2016;103:8–14. https://doi.org/10.1016/j.conbuildmat.2015.11.028.
[45] Sadiqul Islam GM, Gupta SD. Evaluating plastic shrinkage and permeability of polypropylene fiber reinforced concrete. Int J Sustain Built Environ 2016;5(2):345–54. https://doi.org/10.1016/j.ijsbe.2016.05.007.
[46] Reig L, Soriano L, Borrachero MV, Monzó J, Payá J. Influence of calcium aluminate cement (CAC) on alkaline activation of red clay brick waste (RCBW). Cem Concr Compos 2016;65:177–85. https://doi.org/10.1016/j.cemconcomp.2015.10.021.
[47] Ahmed HU, Mohammed AS, Faraj RH, Qaidi SMA, Mohammed AA. Compressive strength of geopolymer concrete modified with nano-silica: Experimental and modeling investigations. Case Stud Constr Mater 2022;16:e01036. https://doi.org/10.1016/j.cscm.2022.e01036.
[48] Ahmed HU, Mohammed AS, Faraj RH, Abdalla AA, Qaidi SM, Sor NH, et al. Innovative modeling techniques including MEP, ANN and FQ to forecast the compressive strength of geopolymer concrete modified with nanoparticles. Neural Comput Appl 2023;35(17):12453–79. https://doi.org/10.1007/s00521-023-08378-3.
[49] Win TT, Prasittisopin L, Nganglumpoon R, Pinthong P, Watmanee S, Tolek W, et al. Chemo-physical mechanisms of high-strength cement composites with suprastructure of graphene quantum dots. Cleaner Mater 2024;11:100229. https://doi.org/10.1016/j.clema.2024.100229.
[50] Win TT, Prasittisopin L, Nganglumpoon R, Pinthong P, Watmanee S, Tolek W, et al. Innovative GQDs and supra-GQDs assemblies for developing high strength and conductive cement composites. Constr Build Mater 2024;421:135693. https://doi.org/10.1016/j.conbuildmat.2024.135693.
[51] Prasittisopin L, Sereewatthanawut I. Dissolution, nucleation, and crystal growth mechanism of calcium aluminate cement. J Sustainable Cem-Based Mater 2019;8(3):180–97. https://doi.org/10.1080/21650373.2018.1558132.
[52] Pacewska B, Nowacka M, Antonovič V, Aleknevičius M. Investigation of early hydration of high aluminate cement-based binder at different ambient temperatures. J Therm Anal Calorim 2012;109(2):717–26. https://doi.org/10.1007/s10973-012-2233-6.
[53] Pacewska B, Nowacka M, Wilińska I, Kubissa W, Antonovich V. Studies on the influence of spent FCC catalyst on hydration of calcium aluminate cements at ambient temperature. J Therm Anal Calorim 2011;105(1):129–40. https://doi.org/10.1007/s10973-011-1303-5.
[54] He R, Nantung T, Olek J, Lu N. Field study of the dielectric constant of concrete: a parameter less sensitive to environmental variations than electrical resistivity. J Build Eng 2023;74:106938. https://doi.org/10.1016/j.jobe.2023.106938.
[55] Antonovič V, Kerienė J, Boris R, Aleknevičius M. The effect of temperature on the formation of the hydrated calcium aluminate cement structure. Procedia Eng 2013;57:99–106. https://doi.org/10.1016/j.proeng.2013.04.015.
[56] Sereewatthanawut I, Prasittisopin L. Effects of accelerating and retarding agents on nucleation and crystal growth of calcium aluminate cement. Open Ceram 2022;11:100290. https://doi.org/10.1016/j.oceram.2022.100290.
[57] Shakor P, Sanjayan J, Nazari A, Nejadi S. Modified 3D printed powder to cement-based material and mechanical properties of cement scaffold used in 3D printing. Constr Build Mater 2017;138:398–409. https://doi.org/10.1016/j.conbuildmat.2017.02.037.
[58] Souza MT, Ferreira IM, de Moraes EG, Senff L, Arcaro S, Pessôa JRC, et al. Role of chemical admixtures on 3D printed Portland cement: Assessing rheology and buildability. Constr Build Mater 2022;314:125666. https://doi.org/10.1016/j.conbuildmat.2021.125666.
[59] Sadakorn W, Prasertsuk S, Prasittisopin L. Improving the structural efficiency of textured three-dimensional concrete printing wall by architectural design. Front Struct Civ Eng 2024:1–17. https://doi.org/10.1007/s11709-024-1001-6.
[60] Lu B, Weng Y, Li M, Qian Y, Leong KF, Tan MJ, et al. A systematical review of 3D printable cementitious materials. Constr Build Mater 2019;207:477–90. https://doi.org/10.1016/j.conbuildmat.2019.02.144.
[61] Prasittisopin L. How 3D printing technology makes cities smarter: a review, thematic analysis, and perspectives. Smart Cities 2024;7(6):3458–88. https://doi.org/10.3390/smartcities7060135.

Thwe Thwe Win [1]Postdoc researcher, Centre of Excellence on Green Tech in Architecture, Department of Architecture, Faculty of Architecture, Chulalongkorn University, Bangkok, Thailand

Yiwei Weng [2]Assistant Professor, Department of Building and Real Estate, Faculty of Construction and Environment, The Hong Kong Polytechnic University, Hong Kong

Lapyote Prasittisopin [3]Associate Professor, Centre of Excellence on Green Tech in Architecture, Department of Architecture, Faculty of Architecture, Chulalongkorn University, Bangkok, Thailand.